

AD-A157 299

CAVITY SHAPE CHARACTERISTICS FOR SUPERCAVITATING
HYDROFOILS(U) MASSACHUSETTS INST OF TECH CAMBRIDGE DEPT
OF OCEAN ENGINEERING S A KINNAS OCT 84 MIT-84-13
N00014-84-K-0067

1/1

UNCLASSIFIED

F/G 20/4

NL



END

FILMED

DTIC



MICROCOPY RESOLUTION TEST CHART
NATIONAL BUREAU OF STANDARDS-1963-A

AD-A157 299

CAVITY SHAPE CHARACTERISTICS
FOR SUPERCAVITATING HYDROFOILS

SPYROS A. KINNAS

DTIC FILE COPY

Report 84-13

DISTRIBUTION STATEMENT A
Approved for public release
Distribution Unlimited

Massachusetts Institute of Technology
Department of Ocean Engineering
Cambridge, MA 02139

DTIC
ELECTE
JUL 19 1986
S

MASSACHUSETTS INSTITUTE OF TECHNOLOGY
DEPARTMENT OF OCEAN ENGINEERING
CAMBRIDGE, MASSACHUSETTS 02139

Report No. 84-13

CAVITY SHAPE CHARACTERISTICS FOR SUPERCAVITATING HYDROFOILS

Spyros A. Kinnas

October 1984

The preparation of this documentation was carried out under the
Naval Sea Systems Command
General Hydromechanics Research Program
Administered by the
David W. Taylor Naval Ship Research and Development Center
Office of Naval Research Contract N00014-84-0067
MIT OSP 94407



Copyright (C) Massachusetts Institute of Technology 1984

Accession For	
NTIS GRA&I	<input checked="checked" type="checkbox"/>
DTIC TAB	<input type="checkbox"/>
Unannounced	<input type="checkbox"/>
Justification	
By	
Distribution/	
Availability Codes	
Dist.	Avail and/or Special
A/1	

REPORT DOCUMENTATION PAGE		READ INSTRUCTIONS BEFORE COMPLETING FORM
1. REPORT NUMBER 84-13	2. GOVT ACCESSION NO. AD-A157299	3. REPORT'S CATALOG NUMBER
4. TITLE (and Subtitle) CAVITY SHAPE CHARACTERISTICS FOR SUPERCAVITATING HYDROFOILS	5. TYPE OF REPORT & PERIOD COVERED TECHNICAL REPORT	6. PERFORMING ORG. REPORT NUMBER
7. AUTHOR(s) SPYROS A. KINNAS	8. CONTRACT OR GRANT NUMBER(s) N00014-84-K-0067	
9. PERFORMING ORGANIZATION NAME AND ADDRESS Department of Ocean Engineering Massachusetts Institute of Technology 77 Mass. Ave., Cambridge, MA 02139	10. PROGRAM ELEMENT, PROJECT, TASK AREA & WORK UNIT NUMBERS	
11. CONTROLLING OFFICE NAME AND ADDRESS David Taylor Naval Ship Research & Development Center Bethesda, MD 20084	12. REPORT DATE October 1984	13. NUMBER OF PAGES 65
14. MONITORING AGENCY NAME & ADDRESS (if different from Controlling Office)	15. SECURITY CLASS. (of this report) UNCLASSIFIED	15a. DECLASSIFICATION/DOWNGRADING SCHEDULE
16. DISTRIBUTION STATEMENT (of this Report) Approved for public release; distribution unlimited		
17. DISTRIBUTION STATEMENT (of the abstract entered in Block 20, if different from Report)		
18. SUPPLEMENTARY NOTES		
19. KEY WORDS (Continue on reverse side if necessary and identify by block number) Cavitation Supercavitating Hydrofoils Cavity shape Hydrofoils		
20. ABSTRACT (Continue on reverse side if necessary and identify by block number) In this work the problem of a supercavitating hydrofoil in linear theory is stated in terms of integral equations of unknown vortex and cavity source distributions. The general problem is decomposed into the camber, the thickness and the angle of attack problems. For each problem the solution is expressed in terms of integrals of the slope of the lower surface of the hydrofoil weighted by known functions. The numerical scheme to compute those integrals.		

20. (continued) has been proved very accurate and insensitive to the variables of the problem. As an application, tables and some cavity plots are given for the NACA $a = 0.8$ meanline series and the NACA Four-digit Wing Sections thickness forms.

Keywords: Cavitation; Cavity shape. ∇

TABLE OF CONTENTS

Abstract	1
List of Figures	2
List of Tables	3
Nomenclature4
Introduction8
1. FORMULATION OF THE PROBLEM	10
2. LINEAR DECOMPOSITION	13
3. SOLUTION TO THE GENERAL SUPERCAVITATING PROBLEM	17
4. CAVITATION NUMBER σ	19
5. CAVITY VOLUME V	21
6. CAVITY SOURCE DISTRIBUTION $\bar{q}(z)$	22
7. CAVITY THICKNESS DISTRIBUTION $h(x)$	25
8. CAVITY CAMBER DISTRIBUTION $c(x)$	25
9. ANALYTICAL SOLUTIONS FOR SOME HYDROFOILS	26
10. NUMERICAL ANALYSIS	29
References	33
APPENDICES	
A. List of Integrals34
B. Asymptotic Behavior of $\bar{q}(z)$ at the Leading and Trailing Edges of the Cavity38
C. Convergence of Numerical Integrations41
D. Supercavitating NACA $a = 0.8$ Meanlines and NACA 00 Thickness Forms	48

ABSTRACT

In this work the problem of a supercavitating hydrofoil in linear theory is stated in terms of integral equations of unknown vortex and cavity source distributions. The general problem is decomposed into the camber, the thickness and the angle of attack problems. For each problem the solution is expressed in terms of integrals of the slope of the lower surface of the hydrofoil weighted by known functions. The numerical scheme to compute those integrals has been proved very accurate and insensitive to the variables of the problem. As an application, tables and some cavity plots are given for the NACA $a = 0.8$ meanline series and the NACA Four-digit Wing Sections thickness forms.

LIST OF FIGURES

	<u>Page</u>
1. Supercavitating Hydrofoil in Linear Theory.....	12
2. Decomposition of the Supercavitating Hydrofoil Problem...	14
3. Change in the Angle of Attack or in the Scale.....	16
4. Special Cases: Flat Plate and Elliptic Foil.....	27
5. Comparison of the Linear to the Non-linear Theory	
Flat Plate at $\alpha = 4^\circ$ ($\ell/c = 1.4$).....	32
6a. Flat Plate at $\alpha = 4^\circ$ ($\ell/c = 1.1 - 1.3$).....	54
6b. Flat Plate at $\alpha = 4^\circ$ ($\ell/c = 1.4 - 1.6$).....	55
6c. Flat Plate at $\alpha = 4^\circ$ ($\ell/c = 1.7 - 2.0$).....	56
7a. NACA $a = 0.8$ ($f_{max}/c = 0.0679$) at $\alpha = \alpha_i$ ($\ell/c = 1.1 - 1.3$).....	57
7b. NACA $a = 0.8$ ($f_{max}/c = 0.0679$) at $\alpha = \alpha_i$ ($\ell/c = 1.4 - 1.6$).....	58
7c. NACA $a = 0.8$ ($f_{max}/c = 0.0679$) at $\alpha = \alpha_i$ ($\ell/c = 1.7 - 2.0$).....	59
8a. NACA 0010 Thickness Form at $\alpha = 0^\circ$ ($\ell/c = 1.1 - 1.3$)..	60
8b. NACA 0010 Thickness Form at $\alpha = 0^\circ$ ($\ell/c = 1.4 - 1.6$)..	61
8c. NACA 0010 Thickness Form at $\alpha = 0^\circ$ ($\ell/c = 1.7 - 2.0$)..	62
9. The Three Elementary Problems for NACA $a = 0.8$ combined with NACA 0010 at $\alpha = 7^\circ$	63
10. Curves of σ Versus ℓ/c for Some Hydrofoils.....	64
11. Curves of V/c^2 Versus ℓ/c for Some Hydrofoils.....	65

LIST OF TABLES

	<u>Page</u>
1. Flat Plate at $\alpha = 1$ rad	
Cavitation Number σ	43
2. Flat Plate at $\alpha = 1$ rad	
Cavity Volume V/c^2	43
3. Flat Plate at $l/c = 1.4$, $\alpha = 1$ rad	
Cavity Source Distribution $\bar{q}(x)$	44
4. Elliptic Foil at $l/c = 2$ ($\epsilon = 1$); $\sigma, V/c^2$	45
5. Elliptic Foil at $l/c = 2$ ($\epsilon = 1$)	
Cavity Source Distribution $\bar{q}(x)$	45
6. Elliptic Foil at $l/c = 2$ ($\epsilon = 1$)	
Cavity Thicknesses h_i 's ($K = 5$ and $K = 10$)....	46
7. Elliptic Foil at $l/c = 2$ ($\epsilon = 1$)	
Cavity Thicknesses h_i 's ($K = 20$).....	47
8. Flat Plate at $\alpha = 4^\circ$; $\sigma, V/c^2$	51
9. NACA a = 0.8 ($f_{max}/c = 0.0679$) at $\alpha = \alpha_i$; $\sigma, V/c^2$	52
10. NACA 0010 Thickness Form at $\alpha = 0^\circ$; $\sigma, V/c^2$	53

NOMENCLATURE

- α : Constant defined as $\alpha = \sqrt{r^2 + 1}$
 b : Constant defined as $b = \sqrt{r^2 - 1}$
 $B(u, z)$: Integral defined in (8.4)
 c : Chord of the hydrofoil
 $C(x)$: Camber distribution of the foil and cavity (see Figure 1)
 C : Constant defined in (9.5)
 C_D : Drag coefficient
 C_L : Lift coefficient
 C_{L_i} : Lift coefficient at $\alpha = \alpha_i$
 C_M : Moment coefficient
 D : Constant defined in (9.5)
 f_{max} : Maximum camber of the hydrofoil
 $f(\theta)$: Function defined in (10.3)
 $F(z)$: Integral defined in (B.5)
 $F_0(z)$: Integral defined in (B.6)
 G : Constant defined in (B.4)
 $h(x)$: Cavity thickness distribution (see Figure 1)
 h_i : Discrete cavity thickness distribution (see also C.1)
 $I(\eta)$: Integral defined as $I(\eta) = \int_0^t \sqrt{\frac{t-z}{z}} \cdot \frac{1}{1+z^2} \cdot \frac{1}{z-\eta} \cdot dz$
 $\bar{I}(z)$: Integral defined in (6.2)
 $J(\eta)$: Integral defined in (5.9)
 K : Number of uniform intervals to apply Simpson's rule
 $\bar{K}(z)$: Integral defined in (6.6)

- ℓ : Cavity length (see Figure 1)
 P_{∞} : Free stream pressure (see Figure 1)
 $P(z)$: Integral defined in (A.21)
 $q(x)$: Cavity source distribution on the cavitating hydrofoil
 (see Figure 1)
 $\bar{q}(x)$: Defined as $\bar{q}(x) = q(x) / (\sigma \cdot V_{\infty})$
 Q : Quantity depending linearly on the solution $\sigma, \gamma(x), q(x)$
 (i.e. $\sigma, \gamma(x), q(x), h(x), c(x), V, C_L, C_M, \sqrt{C_D}$)
 r : Constant defined as $r = \left(\frac{\ell}{\ell-1}\right)^{1/4}$ or $r = (1+t^2)^{1/4}$
 $R(\omega, z)$: Integral defined in (6.7)
 $S(z)$: Integral defined in (A.20)
 t : Constant defined as $t = 1/\sqrt{\ell-1}$
 t_{max} : Maximum thickness of the hydrofoil
 u : x -component of the perturbation velocity (see Figure 1)
 V_{∞} : Free stream velocity (see Figure 1)
 V : y -component of the perturbation velocity (see Figure 1)
 $v(x)$: Induced velocity in wake by the vorticity distribution $\gamma(x)$
 $\bar{v}(x)$: Defined as $\bar{v}(x) = v(x) / (\sigma \cdot V_{\infty})$
 V : Cavity volume (including the foil)
 (x, y) : Coordinate system for the hydrofoil (see Figure 1)
 $\gamma_c(x)$: Camber distribution of the hydrofoil (see Figure 1)
 $\gamma_t(x)$: Thickness distribution of the hydrofoil (see Figure 2)
 z : Transformed x defined as $z = \sqrt{\frac{x}{\ell-x}}$; $0 \leq z \leq t$

α : Angle of attack

α_i : Ideal angle of attack

$\gamma(x)$: Vortex distribution on the cavitating hydrofoil

(see Figure 1)

$\bar{\gamma}(x)$: Defined as $\bar{\gamma}(x) = \gamma(x) / (\sigma \cdot V_\infty)$

$\Delta\alpha$: Increment in the angle of attack α

ε : Similarity parameter

η : Transformed ξ defined as $\eta = \sqrt{\frac{\xi}{\ell - \xi}}$; $0 \leq \eta \leq t$

$\bar{\eta}(x)$: Distribution of the lower surface of the hydrofoil

(see Figure 1)

ϑ : Transformed η defined by the relationship:

$$\eta = t \cdot \sin^2\left(\frac{\vartheta}{2}\right) ; \quad 0 \leq \vartheta \leq \pi$$

$\vartheta^*(x)$: Defined as $\vartheta^*(x) = \frac{1}{\sigma} \cdot \frac{\partial \bar{\eta}}{\partial x}$

ξ : Same as x

ρ_L : Radius of curvature at the leading edge of the hydrofoil

σ : Cavitation number; $\sigma = (p_\infty - p_v) / \left(\frac{\rho}{2} \cdot V_\infty^2\right)$

p_v : vapor pressure

ρ : density of the fluid

$\Phi(\eta, \omega)$: Integral defined in (6.4)

ϕ : Transformed ξ defined by the relationship:

$$\xi = \ell \cdot \sin^2\left(\frac{\phi}{2}\right) ; \quad 0 \leq \phi \leq \pi$$

ω : Same as η

Subscripts

- c : Refers to camber problem (see Figure 3)
- t : Refers to thickness problem (see Figure 3)
- α : Refers to flat plate problem at angle of attack α
(see Figure 3)

$$\sigma = \frac{4\sqrt{2}r^4}{\pi(r^2+1)} \cdot \int_0^t \sqrt{\frac{\eta}{t-\eta}} \cdot \frac{1}{(1+\eta^2)^2} \cdot (a+b\eta) \cdot \left(-\frac{\partial \bar{\eta}}{\partial x}\right) \cdot d\eta \quad (4.9)$$

where:

$$\begin{aligned} r^4 &= 1 + t^2 \\ t^2 &= 1/(\ell-1) \end{aligned} \quad (4.10)$$

Equation (4.9) gives σ in terms of an integral of the slope $\frac{\partial \bar{\eta}}{\partial x}$ of the lower surface of the hydrofoil and functions of ℓ . The numerical implementation of (4.9) for a general shape hydrofoil is described in §10. Equivalent expressions for σ but also for C_L , C_M and C_D have first been given by Hanaoka in [1].

In this work, we focus more on the cavity shape than on the hydrodynamic characteristics of the cavitating hydrofoil. Thus we proceed by giving general expressions for the cavity volume V and the cavity source distribution $q(x)$.

5. CAVITY VOLUME V

The cavity volume V will be given by the expression

$$\begin{aligned} V &= \int_0^\ell h(x) \cdot dx = x \cdot h(x) \Big|_0^\ell - \int_0^\ell x \cdot \frac{dh}{dx} \cdot dx = \\ &= - \int_0^\ell x \cdot \frac{q(x)}{v_\infty} \cdot dx = -\sigma \cdot \int_0^\ell x \cdot \bar{q}(x) \cdot dx \end{aligned} \quad (5.1)$$

where we have made use of (1.4), (1.10), (3.1)

Now plugging (3.6) in (5.1), by changing the order of integration and by using A.11, A.12 and (4.4), we get:

$$\begin{aligned} \frac{V}{\sigma} &= \int_0^\ell x \cdot \sqrt{\frac{x}{\ell-x}} \cdot dx - \frac{1}{\pi} \cdot \int_0^\ell x \cdot \sqrt{\frac{x}{\ell-x}} \cdot dx \left\{ \int_0^1 \sqrt{\frac{\ell-\xi}{\xi}} \cdot \frac{\bar{\sigma}(\xi) \cdot d\xi}{x-\xi} \right\} = \\ &= \frac{3\pi \cdot \ell^2}{8} - \frac{1}{\pi} \cdot \int_0^1 \bar{\sigma}(\xi) \cdot d\xi \cdot \sqrt{\frac{\ell-\xi}{\xi}} \cdot \left\{ \int_0^\ell x \cdot \sqrt{\frac{x}{\ell-x}} \cdot \frac{1}{x-\xi} \cdot dx \right\} = \end{aligned}$$

$$\text{or } -\frac{\pi}{2} + \int_0^t \frac{2}{(1+\eta^2)^2} \cdot \bar{g}(\eta) \cdot d\eta = 0, \quad (4.5)$$

using the transformation (3.8).

By plugging (3.10) in (4.5) and changing the order of integration we get:

$$\begin{aligned} & -\frac{\pi}{2} + \int_0^t -\frac{2}{\pi} \cdot \sqrt{\frac{t-z}{z}} \cdot \frac{1}{(1+z^2)} \cdot dz \int_0^t \sqrt{\frac{\eta}{t-\eta}} \cdot \left[\frac{\eta}{2} - g^* \right] \cdot \frac{d\eta}{(1+\eta^2)(z-\eta)} = \\ & = -\frac{\pi}{2} - \frac{2}{\pi} \cdot \int_0^t \frac{d\eta}{1+\eta^2} \cdot \sqrt{\frac{\eta}{t-\eta}} \cdot \left[\frac{\eta}{2} - g^* \right] \cdot \int_0^t \sqrt{\frac{t-z}{z}} \cdot \frac{1}{1+z^2} \cdot \frac{1}{z-\eta} \cdot dz = \\ & = -\frac{\pi}{2} - \frac{2}{\pi} \cdot \int_0^t \frac{d\eta}{1+\eta^2} \cdot \sqrt{\frac{\eta}{t-\eta}} \cdot \left[\frac{\eta}{2} - g^* \right] \cdot I(\eta) = 0 \end{aligned} \quad (4.6)$$

Where:

$$I(\eta) = \int_0^t \sqrt{\frac{t-z}{z}} \cdot \frac{1}{1+z^2} \cdot \frac{1}{z-\eta} \cdot dz$$

$$\text{But: } I(\eta) = -\frac{\pi}{\sqrt{2} \cdot (1+\eta^2)} \cdot (\alpha + b \cdot \eta) \quad (\text{see A. 17})$$

$$\text{with: } \alpha = \sqrt{\sqrt{1+t^2} + 1}, \quad b = \sqrt{\sqrt{1+t^2} - 1} \quad (4.7)$$

Therefore the closure condition (4.6) becomes:

$$\frac{\pi}{2} - \sqrt{2} \cdot \int_0^t \sqrt{\frac{\eta}{t-\eta}} \cdot \frac{1}{(1+\eta^2)^2} \cdot \left[\frac{\eta}{2} - g^* \right] \cdot (\alpha + b \cdot \eta) \cdot d\eta = 0 \quad (4.8)$$

And by using equations A.5, A.6 and 3.1 we finally get:

Kutta-condition (3.4).

By plugging (3.8) in (3.6) we get:

$$\bar{q}(z) = -z + \frac{2}{\pi} \cdot z \cdot (1+z^2) \cdot \int_0^1 \frac{\bar{\gamma}(\eta) d\eta}{(z^2-\eta^2) \cdot (1+\eta^2)} \quad (3.11)$$

The expressions (3.10) and (3.11) give the formal solution to our problem as soon as we determine the corresponding cavitation number σ .

4. CAVITATION NUMBER σ

The closure condition (3.5) by using the expression of $\bar{q}(x)$ from (3.6), becomes:

$$-\int_0^l \sqrt{\frac{x}{l-x}} \cdot dx + \frac{1}{\pi} \cdot \int_0^l \sqrt{\frac{x}{l-x}} \cdot dx \cdot \int_0^1 \sqrt{\frac{l-\xi}{\xi}} \cdot \frac{\bar{\gamma}(\xi) \cdot d\xi}{x-\xi} = 0 \quad (4.1)$$

$$\text{But: } \int_0^l \sqrt{\frac{x}{l-x}} \cdot dx = \frac{\pi \cdot l}{2} \quad (\text{see A.10})$$

Therefore:

$$-\frac{\pi \cdot l}{2} + \frac{1}{\pi} \cdot \int_0^l \sqrt{\frac{x}{l-x}} \cdot dx \cdot \int_0^1 \sqrt{\frac{l-\xi}{\xi}} \cdot \frac{\bar{\gamma}(\xi) \cdot d\xi}{x-\xi} = 0 \quad (4.2)$$

or:

$$-\frac{\pi \cdot l}{2} + \frac{1}{\pi} \cdot \int_0^1 d\xi \cdot \sqrt{\frac{l-\xi}{\xi}} \cdot \bar{\gamma}(\xi) \cdot \left(\int_0^l \sqrt{\frac{x}{l-x}} \cdot \frac{1}{x-\xi} \cdot dx \right) = 0, \quad (4.3)$$

by changing the order of integration in the double integral of (4.2).

$$\text{But: } \int_0^l \sqrt{\frac{x}{l-x}} \cdot \frac{1}{x-\xi} \cdot dx = \pi \quad (\text{see A.13a})$$

$$\text{Thus: } -\frac{\pi \cdot l}{2} + \int_0^1 d\xi \cdot \sqrt{\frac{l-\xi}{\xi}} \cdot \bar{\gamma}(\xi) = 0 \quad (4.4)$$

$$-\frac{\bar{q}(x)}{2} + \frac{1}{2\pi} \cdot \int_0^1 \frac{\bar{\sigma}(\xi) \cdot d\xi}{\xi - x} = \mathcal{V}^*(x) ; \quad 0 < x < 1 \quad (3.3)$$

$$\bar{\gamma}(1) = 0 \quad (3.4)$$

$$\int_0^l \bar{q}(x) \cdot dx = 0 \quad (3.5)$$

Using similar procedures as in [1] and [2] we derive the solution to the system of singular integral equations (3.2)-(3.5) as follows:

Inverting first (3.2) we get:

$$\bar{q}(x) = -\sqrt{\frac{x}{l-x}} + \frac{1}{\pi} \cdot \sqrt{\frac{x}{l-x}} \cdot \int_0^1 \sqrt{\frac{l-\xi}{\xi}} \cdot \frac{\bar{\sigma}(\xi) \cdot d\xi}{x-\xi} \quad (3.6)$$

Notice that this is the unique solution which behaves like $\frac{1}{\sqrt{l-x}}$ at the trailing edge of the cavity (T.Y. Wu's singularity).

Plugging (3.6) in (3.3) we finally get:

$$\frac{1}{2\pi} \cdot \int_0^1 \left(\sqrt{\frac{l-x}{x}} + \sqrt{\frac{l-\xi}{\xi}} \right) \cdot \frac{\bar{\sigma}(\xi) \cdot d\xi}{x-\xi} = \frac{1}{2} - \mathcal{V}^*(x) \cdot \sqrt{\frac{l-x}{x}} \quad (3.7)$$

Using the transformation:

$$z^2 = \frac{x}{l-x} \quad , \quad \eta^2 = \frac{\xi}{l-\xi} \quad , \quad t^2 = \frac{1}{l-1} \quad (3.8)$$

(3.7) becomes:

$$\frac{1}{2\pi} \cdot \int_0^t \frac{\bar{\sigma}(\eta) \cdot d\eta}{(1+\eta^2) \cdot (z-\eta)} = \frac{1}{4} \cdot \frac{z}{1+z^2} - \frac{\mathcal{V}^*(x)}{2} \cdot \frac{1}{1+z^2} \quad (3.9)$$

Inversion of the (3.9) gives:

$$\bar{\sigma}(z) = -\frac{1}{\pi} \cdot (1+z^2) \cdot \sqrt{\frac{t-z}{z}} \cdot \int_0^t \sqrt{\frac{\eta}{t-\eta}} \cdot \left[\frac{\eta}{2} - \mathcal{V}^*(\eta) \right] \frac{d\eta}{(1+\eta^2) \cdot (z-\eta)} \quad (3.10)$$

Notice that (3.10) gives the unique solution which satisfies also the

cavity length (see Fig. 3a).

b) Affine camber meanlines and thickness forms

$$Q_f = \varepsilon \cdot Q_{f_0} \quad (2.8)$$

where Q_f and Q_{f_0} correspond to camber/chord ratios f and f_0 respectively and zero angle of attack (see Fig 3b).

A similar relationship is also true for affine thickness forms.

Therefore for a given camber or thickness series we need to solve the problem for one value of the similarity parameter and one angle of attack.

The decomposition described above can also be done when the cavity does not start at the leading edge of the foil. In that case both the leading edge and the trailing edge of the cavity have to remain fixed for each elementary problem.

3. SOLUTION TO THE GENERAL SUPERCAVITATING PROBLEM

It is convenient to non-dimensionalize equations (1.6)-(1.9) by dividing by $(\sigma \cdot V_\infty)$ and calling

$$\bar{\gamma}(x) = \frac{\gamma(x)}{\sigma \cdot V_\infty}, \quad \bar{q}(x) = \frac{q(x)}{\sigma \cdot V_\infty}, \quad \gamma^*(x) = \frac{1}{\sigma} \cdot \frac{\partial \bar{\gamma}}{\partial x} \quad (3.1)$$

$$\frac{\bar{\gamma}(x)}{2} - \frac{1}{2\pi} \cdot \int_0^e \frac{\bar{q}(\xi) \cdot d\xi}{\xi - x} = \frac{1}{2} \quad ; \quad 0 < x < e \quad (3.2)$$

with $\bar{\gamma}(x) = 0$ for $1 < x < e$

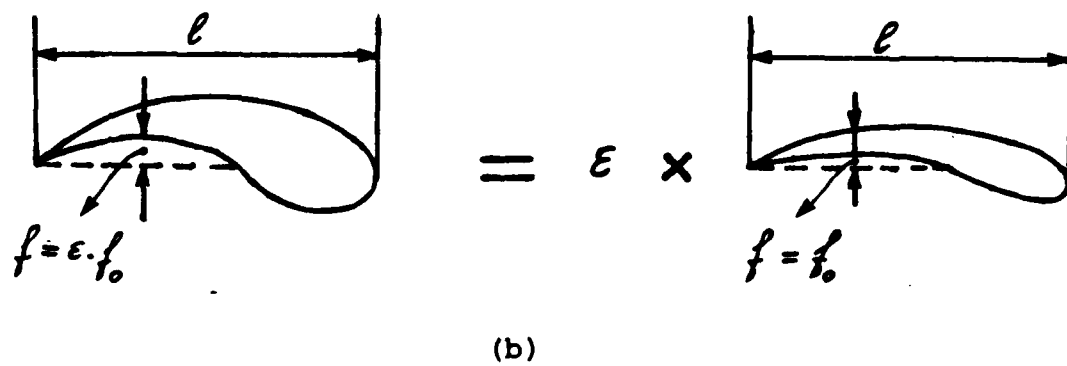
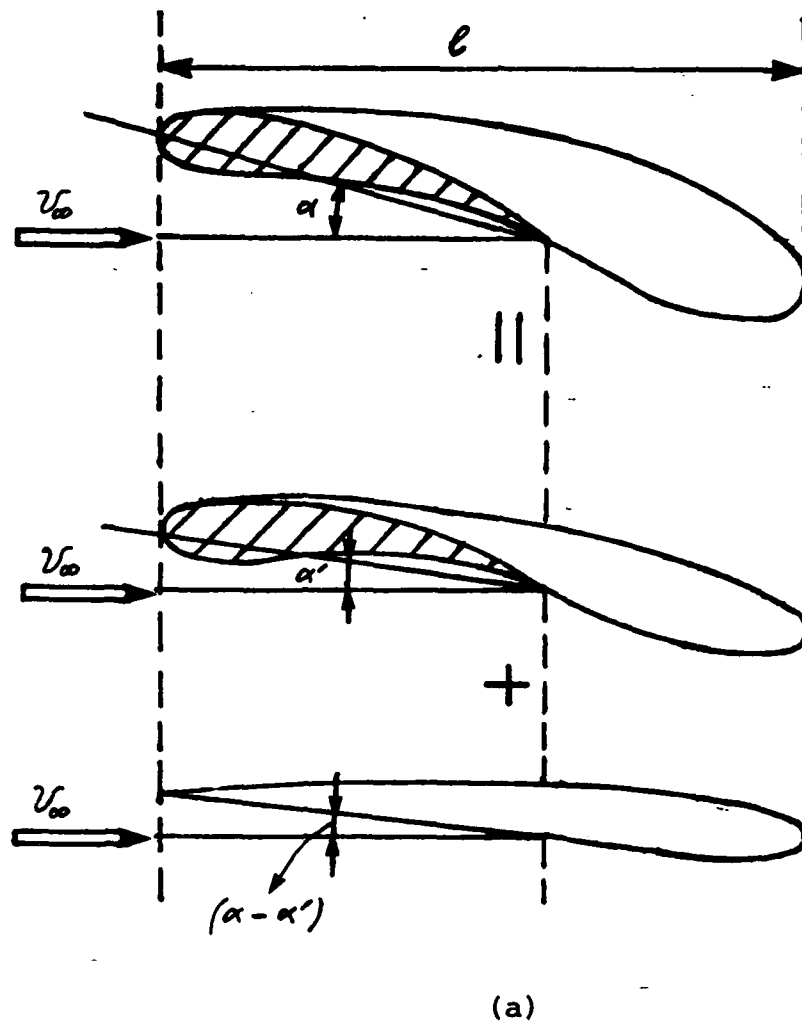


Figure 3
CHANGE IN THE ANGLE OF ATTACK OR IN THE SCALE

- a) Camber problem with $\bar{\eta}(x) = \gamma_c(x)$
- b) Thickness problem with $\bar{\eta}(x) = -\gamma_t(x)$
- c) Flat plate at angle of attack α

The solution $\sigma, \gamma(x), q(x)$ will be the linear superposition of the solutions of those problems:

$$\sigma = \sigma_c + \sigma_t + \sigma_\alpha \quad (2.3)$$

$$\gamma(x) = \gamma_c(x) + \gamma_t(x) + \gamma_\alpha(x). \quad (2.4)$$

$$q(x) = q_c(x) + q_t(x) + q_\alpha(x) \quad (2.5)$$

Furthermore, for each quantity Q which depends linearly on the solution, we will have:

$$Q = Q_c + Q_t + Q_\alpha \quad (2.6)$$

For example Q can be: $\sigma, \gamma(x), q(x), h(x), c(x), V, c_L, c_M, \sqrt{C_D}$

Some particular cases can then be examined:

- a) Change of angle of attack

$$Q = Q' + Q(\alpha - \alpha') \quad (2.7)$$

where Q' corresponds at angle of attack α' .

In other words if we change the angle of attack by $\Delta\alpha$ then the solution for the same cavity length will change by an amount which is the solution to a flat plate at angle of attack $\Delta\alpha$ and the same

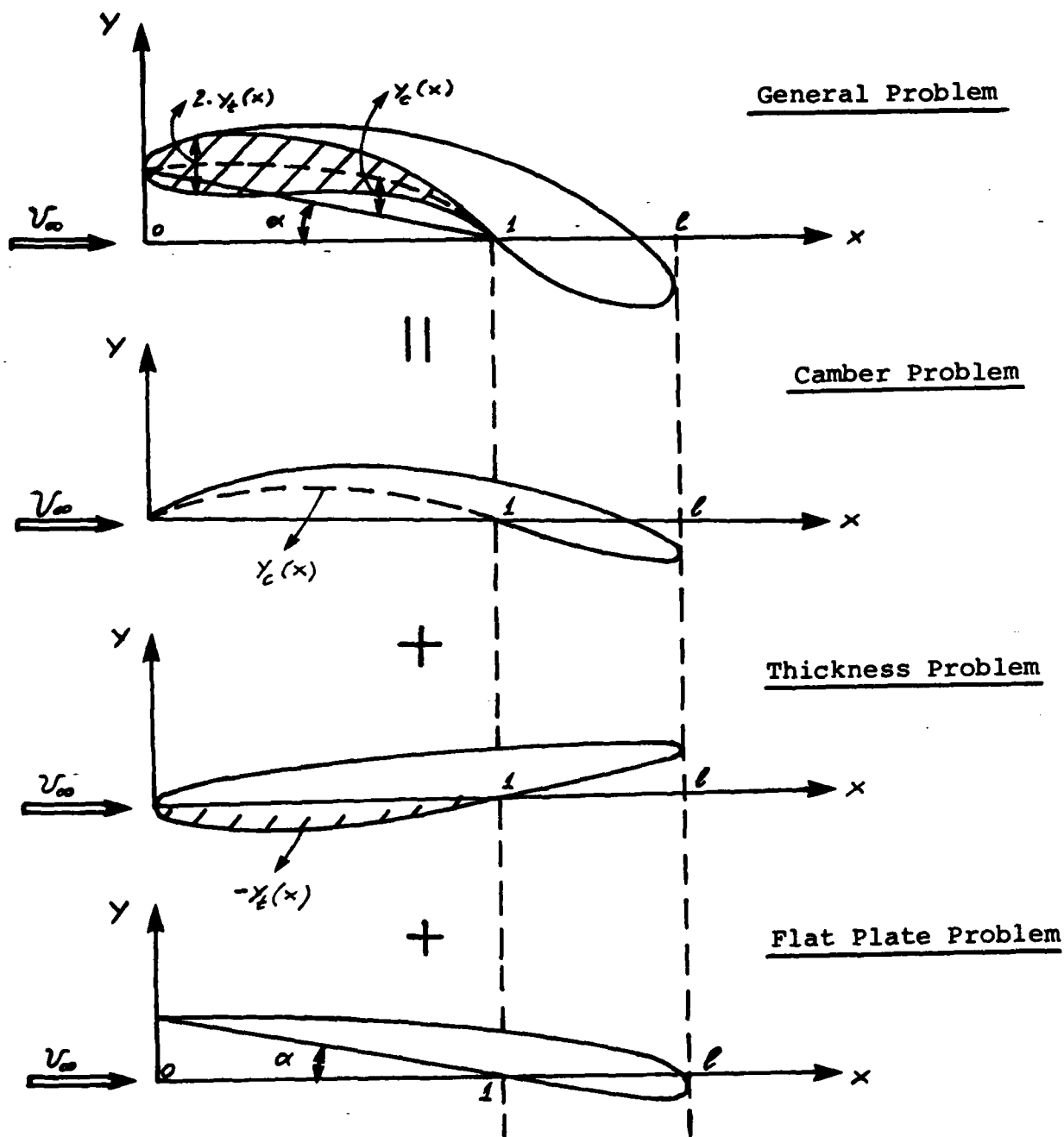


Figure 2

DECOMPOSITION OF THE SUPERCAVITATING HYDROFOIL PROBLEM

The cavity thickness $h(x)$ and the cavity camber $c(x)$ will then be given by the following relationships:

$$V_{\infty} \cdot \frac{\partial h}{\partial x} = q(x) \quad ; \quad 0 < x < \ell \quad (1.10)$$

$$c(x) = \bar{\eta}(x) + \frac{h(x)}{2} \quad ; \quad 0 < x < 1 \quad (1.11a)$$

$$V_{\infty} \cdot \frac{\partial c}{\partial x} = v(x) \quad ; \quad 1 < x < \ell \quad (1.11b)$$

$$v(x) = -\frac{1}{2\pi} \cdot \int_0^1 \frac{\gamma(\xi) \cdot d\xi}{x - \xi} \quad ; \quad 1 < x < \ell \quad (1.12)$$

$v(x)$: induced velocity in the wake by the vorticity distribution $\gamma(x)$

2. LINEAR DECOMPOSITION

If the hydrofoil has a camber meanline $\gamma_c(x)$, a thickness distribution $2 \cdot \gamma_t(x)$ and an angle of attack α , then the lower surface will be: (see Fig. 2)

$$\bar{\eta}(x) = \gamma_c(x) - \gamma_t(x) + \alpha \cdot (1-x) \quad (2.1)$$

and

$$\frac{\partial \bar{\eta}}{\partial x} = \frac{\partial \gamma_c}{\partial x} - \frac{\partial \gamma_t}{\partial x} - \alpha \quad (2.2)$$

From equations (1.6)-(1.9), it is easily seen that as long as we keep ℓ fixed then the supercavitating general shape hydrofoil problem can be considered as the superposition of the following three elementary problems: (see Fig. 2)

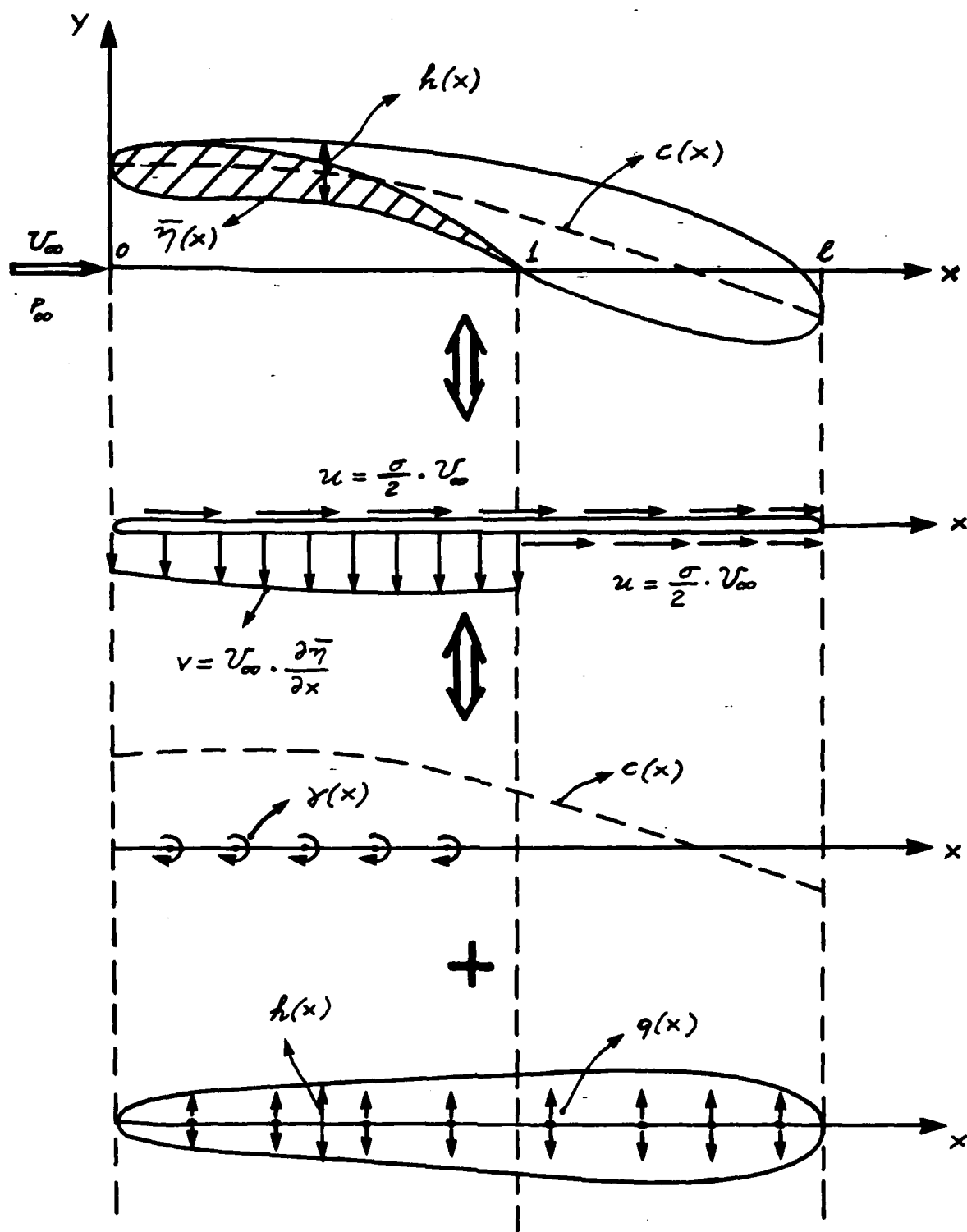


Figure 1

SUPERCAVITATING HYDROFOIL IN LINEAR THEORY

(u, v) finite at $x = 1$

d) Closure condition

Cavity thickness at the trailing edge of the cavity, $h(\ell) = 0$

(1.4)

e) Condition at infinity

$u \rightarrow 0$ and $v \rightarrow 0$ at infinity

(1.5)

The boundary conditions in terms of the unknown distributions

$\gamma(x)$ and $q(x)$, will become:

$$\frac{\gamma(x)}{2} - \frac{1}{2\pi} \int_0^\ell \frac{q(\xi) \cdot d\xi}{\xi - x} = \frac{\sigma}{2} \cdot v_\infty \quad ; \quad 0 < x < \ell \quad (1.6)$$

with $\gamma(x) = 0$ for $1 < x < \ell$

$$-\frac{q(x)}{2} + \frac{1}{2\pi} \int_0^1 \frac{\gamma(\xi) \cdot d\xi}{\xi - x} = v_\infty \cdot \frac{\partial \bar{\eta}}{\partial x} \quad ; \quad 0 < x < 1 \quad (1.7)$$

$$\gamma(1) = 0 \quad (1.8)$$

$$\int_0^\ell q(x) \cdot dx = 0 \quad (1.9)$$

The boundary condition (1.5) is automatically satisfied by the use of vortices and sources for the representation of the velocity field. For given ℓ and $\bar{\eta}(x)$, the equations (1.6) - (1.9) give us the unique solution $\sigma, \gamma(x)$ and $q(x)$.

1. FORMULATION OF THE PROBLEM

Consider a supercavitating hydrofoil of chord l . in uniform flow V_∞ and ambient pressure p_∞ (see Fig. 1.). Given the cavity length ℓ and the lower surface $\bar{\eta}(x)$ of the hydrofoil we want to determine the corresponding cavitation number σ and the shape of the cavity.

According to the linear theory the perturbation velocity field (components u and v) due to the cavity and the foil can be generated by a distribution of vortices $\gamma(x)$ and sources $q(x)$, along the slit from $x=0$ to $x=\ell$ (see Fig. 1.).

The linearized boundary conditions are (throughout our analysis, we assume that the cavity starts at the leading edge of the foil):

a) Dynamic boundary conditions

$$u = \frac{\sigma}{2} \cdot V_\infty \quad ; \quad 0 < x < \ell, \quad y = 0^+ \quad (1.1)$$

$$u = \frac{\sigma}{2} \cdot V_\infty \quad ; \quad 1 < x < \ell, \quad y = 0^- \quad (1.2)$$

b) Kinematic boundary condition

$$v = V_\infty \cdot \frac{\partial \bar{\eta}}{\partial x} \quad ; \quad 0 < x < 1, \quad y = 0^- \quad (1.3)$$

c) Kutta condition

compact than the ones given by the previous authors. He also gave series representations for his results when the hydrofoil shape could be expressed in terms of polynomials of the chordwise coordinate.

In this work, the linear problem is stated in a simple way but equivalent to the one described in [1], in terms of integral equations of cavity source and vortex distributions. The principle of decomposition, first introduced by Fabula for a hydrofoil with cut-off ventilated trailing edge [11] and for a supercavitating hydrofoil at different angles of attack [12], is extended to our problem which is divided into the camber, the thickness and the angle of attack problems. Formulas for the cavitation number, the cavity volume and the cavity source distribution, are given in terms of integrals of the lower surface of the hydrofoil weighted by known functions. These integrals are computed numerically using Simpson's rule with respect to an appropriate transformation variable, thus avoiding the involved singularities of the integrands. The cavity shape is also computed numerically. The results for a flat plate and an elliptic foil, for which analytical solutions are available, seem to be very accurate even for a small number of the used intervals in the numerical integrations. The cavity shape for a flat plate is compared to the nonlinear result given by Uhlman [5], and is found to be very close except at the trailing edge of the cavity.

Finally, the proposed method is applied for the NACA $a = 0.8$ meanline series and the NACA Four-digit Wing Sections thickness forms for which tables and some cavity plots are given.

INTRODUCTION

The problem of a supercavitating hydrofoil in uniform flow has received a lot of attention in the past three decades, individually as well as a first step towards the understanding of the phenomenon of cavitating marine propellers.

The non-linear formulation of the problem is not unique due to the variety of the cavity termination models. Furthermore, the non-linear problem is very difficult to deal with analytically, especially for general shape hydrofoils.

Linear theory was first applied by Tulin [8] to the problem of a supercavitating flat plate at small angles and arbitrary cavitation numbers. It was subsequently extended by T.Y. Wu [9], Geurst [3], Parkin [10] and Fabula [12] for a supercavitating hydrofoil of general shape. These authors have worked by means of the complex velocity function, and have given expressions for the cavitation number, the hydrodynamic coefficients and the cavity volume, in terms of integrals of known quantities.

Hanaoka [1] stated the linear problem in terms of integral equations of unknown distributions of sources and dipoles on the foil. Inversion of these integral equations produced integral representations for the cavitation number, the hydrodynamic coefficients and the slope of the upper and lower cavity surfaces in terms of the shape of the hydrofoil. His formulas are less complicated and more

$$= \frac{\pi \cdot \ell^2}{8} - \int_0^t \bar{\sigma}(\xi) \cdot \xi \cdot \sqrt{\frac{\ell - \xi}{\xi}} \cdot d\xi \quad (5.2)$$

Casting (5.2) in terms of (3.8) we have:

$$\begin{aligned} \frac{V}{\sigma} &= \frac{\pi \cdot \ell^2}{8} + \frac{2\ell^2}{\pi} \cdot \int_0^t \frac{z^2}{(1+z^2)^2} \cdot \sqrt{\frac{t-z}{z}} \cdot dz \int_0^t \sqrt{\frac{\eta}{t-\eta}} \cdot \left[\frac{\eta}{2} - \vartheta^* \right] \cdot \frac{d\eta}{(1+\eta^2) \cdot (z-\eta)} = \\ &= \frac{\pi \cdot \ell^2}{8} + \frac{2\ell^2}{\pi} \cdot \int_0^t \left[\frac{\eta}{2} - \vartheta^* \right] \cdot \sqrt{\frac{\eta}{t-\eta}} \cdot \frac{1}{(1+\eta^2)} \cdot \mathcal{J}(\eta) \cdot d\eta \end{aligned} \quad (5.8)$$

where

$$\mathcal{J}(\eta) = \int_0^t \frac{z^2}{(1+z^2)^2} \cdot \sqrt{\frac{t-z}{z}} \cdot \frac{1}{z-\eta} \cdot dz \quad (5.9)$$

Now $\mathcal{J}(\eta)$ can be expressed in terms of η and ℓ as follows

(see A.18)

$$\begin{aligned} \mathcal{J}(\eta) &= \frac{\pi}{\sqrt{2} \cdot r^2} \cdot \frac{1}{1+\eta^2} \cdot \left[\frac{\eta(t-\eta)}{1+\eta^2} \cdot \left\{ \sqrt{r^2+1} - \eta \cdot \sqrt{r^2-1} \right\} - \right. \\ &\quad - \frac{(1+\eta \cdot t)}{4 \cdot r^6} \cdot \left\{ 2 \cdot t^2 \cdot \sqrt{r^2+1} + t \cdot (t^2-1) \cdot \sqrt{r^2-1} \right\} + \\ &\quad \left. + \frac{(t-\eta)}{4 \cdot r^6} \cdot \left\{ t \cdot (t^2+3) \cdot \sqrt{r^2+1} - 2 \cdot \sqrt{r^2-1} \right\} \right] \end{aligned} \quad (5.10)$$

And finally the cavity volume is given in terms of $\frac{\partial \bar{\eta}}{\partial x}$, σ

and ℓ as:

$$V = \ell^2 \cdot \left\{ \frac{\pi \cdot \sigma}{8} - \frac{2}{\pi} \cdot \int_0^t \left[\frac{\sigma \cdot \eta}{2} - \frac{\partial \bar{\eta}}{\partial x} \right] \cdot \sqrt{\frac{\eta}{t-\eta}} \cdot \frac{1}{1+\eta^2} \cdot \mathcal{J}(\eta) \cdot d\eta \right\} \quad (5.11)$$

6. CAVITY SOURCE DISTRIBUTION $\bar{q}(z)$

Starting from equation (3.11) and plugging in the expression for $\bar{\sigma}$

from (3.10), we get:

$$\bar{q}(z) = -z + \frac{z}{\pi} \cdot 2 \cdot (1+z^2) \cdot \int_0^t \frac{\bar{\sigma}(\eta) \cdot d\eta}{(z^2-\eta^2) \cdot (1+\eta^2)} =$$

$$= -z - \frac{2z}{\pi^2} \cdot (1+z^2) \cdot \int_0^t \sqrt{\frac{t-\eta}{\eta}} \cdot \frac{1}{(z^2-\eta^2)} \cdot d\eta \int_0^t \sqrt{\frac{\omega}{t-\omega}} \cdot \left[\frac{\omega}{2} - \vartheta^*(\omega) \right] \cdot \frac{d\omega}{(1+\omega^2)(\eta-\omega)} \quad (6.1)$$

We call the double integral in (6.1) $\bar{I}(z)$:

$$\bar{I}(z) = \int_0^t \sqrt{\frac{t-\eta}{\eta}} \cdot \frac{1}{z^2-\eta^2} \cdot d\eta \int_0^t \sqrt{\frac{\omega}{t-\omega}} \cdot \left[\frac{\omega}{2} - \vartheta^*(\omega) \right] \cdot \frac{d\omega}{(1+\omega^2)(\eta-\omega)} \quad (6.2)$$

or:

$$\bar{I}(z) = \int_0^t \frac{d\eta}{\eta-z} \cdot \int_0^t \frac{\Phi(\eta, \omega)}{\omega-\eta} \cdot d\omega \quad (6.3)$$

where:

$$\Phi(\eta, \omega) = \sqrt{\frac{t-\eta}{\eta}} \cdot \frac{1}{z+\eta} \cdot \sqrt{\frac{\omega}{t-\omega}} \cdot \left[\frac{\omega}{2} - \vartheta^*(\omega) \right] \cdot \frac{1}{(1+\omega^2)} \quad (6.4)$$

Now, to change the order of integration in (6.3) we apply

Poincaré-Bertrand's formula:

$$\bar{I}(z) = \int_0^t d\omega \int_0^t \frac{\Phi(\eta, \omega)}{(\eta-z)(\omega-\eta)} \cdot d\eta \quad ; \quad z \geq t \quad (6.5a)$$

$$\bar{I}(z) = \int_0^t d\omega \int_0^t \frac{\Phi(\eta, \omega)}{(\eta-z)(\omega-\eta)} \cdot d\eta - \pi^2 \cdot \Phi(z, z) \quad ; \quad z < t \quad (6.5b)$$

We then focus on the integral:

$$\begin{aligned} \bar{K}(z) &= \int_0^t d\omega \int_0^t \frac{\Phi(\eta, \omega)}{(\eta-z)(\omega-\eta)} \cdot d\eta = \\ &= \int_0^t d\omega \cdot \sqrt{\frac{\omega}{t-\omega}} \cdot \frac{1}{1+\omega^2} \cdot \left[\frac{\omega}{2} - \vartheta^* \right] \cdot \left\{ \int_0^t \sqrt{\frac{t-\eta}{\eta}} \cdot \frac{1}{z^2-\eta^2} \cdot \frac{1}{\eta-\omega} \cdot d\eta \right\} \end{aligned} \quad (6.6)$$

and we call:

$$R(\omega, z) = \int_0^t \sqrt{\frac{t-\eta}{\eta}} \cdot \frac{1}{z^2-\eta^2} \cdot \frac{1}{\eta-\omega} \cdot d\eta \quad (6.7)$$

But $R(\omega, z)$ can be expressed explicitly as: (see A.19)

$$R(\omega, z) = -\frac{\pi}{2 \cdot z \cdot (z+\omega)} \cdot \left(\frac{t+z}{z} \right)^{1/2} \quad ; \quad z \leq t \quad (6.8a)$$

$$R(\omega, z) = -\frac{\pi}{2 \cdot z \cdot (z+\omega)} \cdot \left(\frac{t+z}{z} \right)^{1/2} - \frac{\pi}{2 \cdot z \cdot (z-\omega)} \cdot \left(\frac{z-t}{z} \right)^{1/2} \quad ; \quad z > t \quad (6.8b)$$

Plugging (6.5) in (6.1) and using (6.6), (6.8), (A.20) and (A.21) we get:

$$\begin{aligned}\bar{q}(z) = & -\vartheta^*(z) + \left(\frac{t+z}{z}\right)^{\frac{1}{2}} \cdot \frac{1}{2\sqrt{2}r^2} \cdot \left(\sqrt{r^2-1} - z\sqrt{r^2+1}\right) - \\ & - \frac{1}{\pi} \cdot (1+z^2) \cdot \left(\frac{t+z}{z}\right)^{\frac{1}{2}} \cdot \int_0^t \sqrt{\frac{\omega}{t-\omega}} \cdot \frac{1}{1+\omega^2} \cdot \frac{\vartheta^*(\omega)}{z+\omega} \cdot d\omega\end{aligned}$$

for $z < t$

(6.9a)

$$\begin{aligned}\bar{q}(z) = & \left(\frac{t+z}{z}\right)^{\frac{1}{2}} \cdot \frac{1}{2\sqrt{2}r^2} \cdot \left(\sqrt{r^2-1} - z\sqrt{r^2+1}\right) - \\ & - \frac{1}{\pi} \cdot (1+z^2) \cdot \left(\frac{t+z}{z}\right)^{\frac{1}{2}} \cdot \int_0^t \sqrt{\frac{\omega}{t-\omega}} \cdot \frac{1}{1+\omega^2} \cdot \frac{\vartheta^*(\omega)}{z+\omega} \cdot d\omega - \\ & - \left(\frac{z-t}{z}\right)^{\frac{1}{2}} \cdot \frac{1}{2\sqrt{2}r^2} \cdot \left(\sqrt{r^2+1} \cdot z + \sqrt{r^2-1}\right) - \\ & - \frac{1}{\pi} \cdot (1+z^2) \cdot \left(\frac{z-t}{z}\right)^{\frac{1}{2}} \cdot \int_0^t \sqrt{\frac{\omega}{t-\omega}} \cdot \frac{1}{1+\omega^2} \cdot \frac{\vartheta^*(\omega)}{z-\omega} \cdot d\omega\end{aligned}$$

for $z \geq t$

(6.9b)

7. CAVITY THICKNESS DISTRIBUTION $h(x)$

Integrating (1.10) and using (3.1), we get:

$$h(x) = \sigma \cdot \int_0^x \bar{q}(\xi) \cdot d\xi \quad (7.1)$$

For the numerical integration of (7.1) see §10.

8. CAVITY CAMBER DISTRIBUTION $c(x)$

The camber meanline of the cavity and foil, $c(x)$, for $0 < x < 1$ is explicitly determined from (1.11a) in terms of the foil characteristics and the cavity thickness $h(x)$. For $1 < x < \ell$ it is going to be determined from (1.11b) after we first express $v(x)$ in terms of $\frac{\partial \bar{\eta}}{\partial x}$ and ℓ :

From the definition (1.12) we get:

$$\bar{v}(x) = -\frac{1}{2\pi} \cdot \int_0^1 \frac{\bar{\sigma}(\xi) \cdot d\xi}{x - \xi} \quad (8.1)$$

where

$$\bar{v}(x) = \frac{v(x)}{\sigma \cdot U_\infty} \quad (8.2)$$

Expressing (8.1) in terms of the transformation (3.8) and then using (3.10) we get:

$$\begin{aligned} \bar{v}(z) &= -\frac{1}{\pi} \cdot (1 + z^2) \cdot \int_0^t \frac{\bar{\sigma}(\eta) \cdot \eta \cdot d\eta}{(1 + \eta^2) \cdot (z^2 - \eta^2)} = \\ &= \frac{1}{\pi^2} \cdot (1 + z^2) \cdot \int_0^t \frac{\eta}{z^2 - \eta^2} \cdot \sqrt{\frac{t - \eta}{\eta}} \cdot d\eta \int_0^t \sqrt{\frac{\omega}{t - \omega}} \cdot \left[\frac{\omega}{2} - \eta^* \right] \cdot \frac{d\omega}{(1 + \omega^2)(\eta - \omega)} = \\ &= \frac{1}{\pi^2} \cdot (1 + z^2) \cdot \int_0^t \sqrt{\frac{\omega}{t - \omega}} \cdot \left[\frac{\omega}{2} - \eta^* \right] \cdot \frac{B(\omega, z) \cdot d\omega}{1 + \omega^2} \quad (8.3) \end{aligned}$$

$$\text{where } B(\omega, z) = \int_0^t \frac{\eta}{z^2 - \eta^2} \cdot \sqrt{\frac{t - \eta}{\eta}} \cdot \frac{1}{\eta - \omega} \cdot d\eta \quad (8.4)$$

Using now A.22, A.20, A.21, we get:

$$\begin{aligned} \bar{v}(z) = & \sqrt{\frac{t+z}{z}} \cdot \frac{1}{4\sqrt{2}r^2} \cdot (\sqrt{r^2-1} - z\sqrt{r^2+1}) + \\ & + \sqrt{\frac{z-t}{z}} \cdot \frac{1}{4\sqrt{2}r^2} \cdot (\sqrt{r^2+1} \cdot z + \sqrt{r^2-1}) - \\ & - \sqrt{\frac{t+z}{z}} \cdot \frac{1}{2\pi} \cdot (1+z^2) \cdot \int_0^t \sqrt{\frac{\omega}{t-\omega}} \cdot \frac{g^*(\omega)}{z+\omega} \cdot \frac{1}{1+\omega^2} \cdot d\omega + \\ & + \sqrt{\frac{z-t}{z}} \cdot \frac{1}{2\pi} \cdot (1+z^2) \cdot \int_0^t \sqrt{\frac{\omega}{t-\omega}} \cdot \frac{g^*(\omega)}{z-\omega} \cdot \frac{1}{1+\omega^2} \cdot d\omega \end{aligned}$$

for $z \geq t$ (8.5)

and by integrating (1.11b) we get:

$$c(x) = c(1) + \sigma \cdot \int_1^x \bar{v}(\xi) \cdot d\xi \quad (8.6)$$

with

$$c(1) = \bar{\eta}(1) + \frac{h(1)}{2} \quad (8.7)$$

9. ANALYTICAL SOLUTIONS FOR SOME HYDROFOILS

9.1 Flat Plate (see Fig. 4a)

For this case we have

$$\frac{\partial \bar{\eta}}{\partial x} = -\alpha \quad (9.1)$$

where α = angle of attack

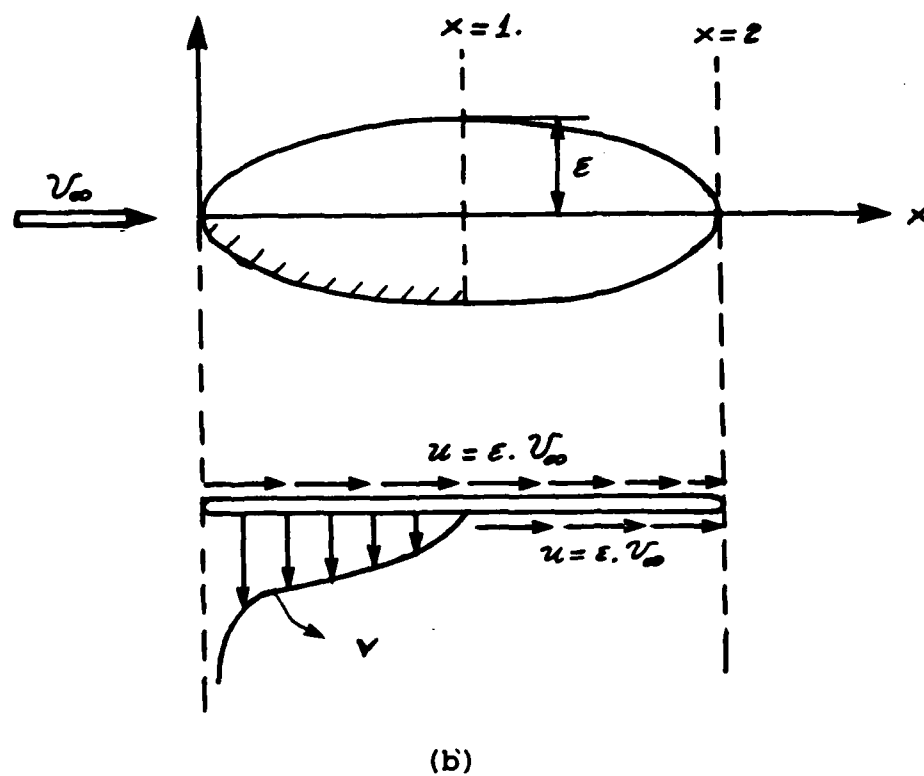
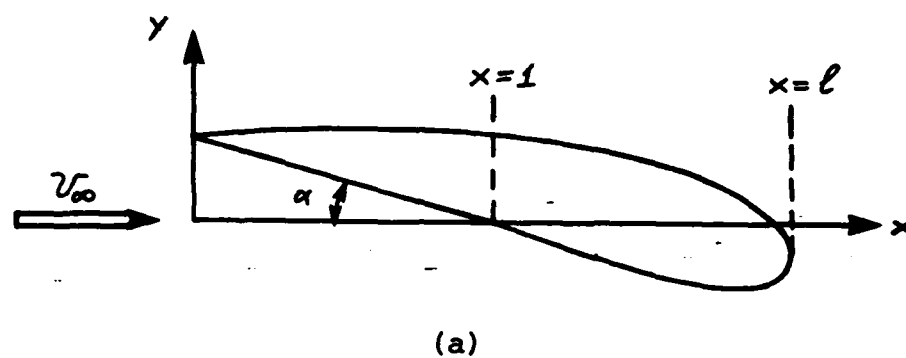


Figure 4

SPECIAL CASES: FLAT PLATE AND ELLIPTIC FOIL

and the expressions (4.9), (6.9), (8.5) by using the formulas in Appendix A reduce to: (see also [2] and [3])

$$\sigma = 2.t. \alpha \quad (9.2)$$

$$\bar{q}(z) = (c - D.z) \cdot \sqrt{\frac{z+t}{z}} \quad ; \quad z < t \quad (9.3a)$$

$$\bar{q}(z) = (c - D.z) \cdot \sqrt{\frac{z+t}{z}} - (c + D.z) \cdot \sqrt{\frac{z-t}{z}} \quad ; \quad z \geq t \quad (9.3b)$$

$$\bar{V}(z) = \frac{1}{2} \cdot (c - D.z) \cdot \sqrt{\frac{z+t}{z}} + \frac{1}{2} (c + D.z) \cdot \sqrt{\frac{z-t}{z}} - \frac{1}{2.t} \quad ; \quad z \geq t \quad (9.4)$$

$$\text{where: } c = \frac{1}{\sqrt{2} \cdot r^2} \cdot \left[\frac{1}{2.t} \cdot \sqrt{1+r^2} + \frac{1}{2} \cdot \sqrt{r^2-1} \right] \quad (9.5)$$

$$\text{and: } D = \frac{1}{\sqrt{2} \cdot r^2} \cdot \left[-\frac{1}{2.t} \cdot \sqrt{r^2-1} + \frac{1}{2} \cdot \sqrt{1+r^2} \right]$$

Also by using (5.11) and (9.1) we must recover the result by Geurst in [3] for the cavity volume V :

$$V = \frac{\pi \cdot \alpha \cdot t}{16} \sqrt{\left(1 - \sqrt{\frac{t-1}{t}}\right)^2} \quad (9.6)$$

9.2 Elliptic Foil

Consider an ellipse of semi-axes $(1, \varepsilon)$ (see Fig. 4b) at uniform inflow V_∞ . According to the linear theory the perturbation velocity on the ellipse will be constant: (see [4])

$$u = \varepsilon \cdot V_\infty \quad (9.7)$$

Therefore, if we consider the lower left part of the ellipse as a supercavitating hydrofoil at cavity length $2 \times \text{chord}$ then the shape of

the cavity will be the rest of the ellipse (in linear theory always), and we will also get by inspection:

$$\sigma = 2 \cdot \varepsilon \quad (9.8)$$

$$V = \pi \cdot \varepsilon \quad (9.9)$$

$$\bar{q}(z) = \frac{1-z^2}{2 \cdot z} \quad ; \quad z > 0 \quad (9.10)$$

$$\bar{v}(z) = 0 \quad ; \quad z \geq t \quad (9.11)$$

Equations (9.8)-(9.11) can also be recovered by plugging in (4.9), (5.11), (6.9) and (8.5) the expression for $\frac{\partial \bar{\eta}}{\partial x}$:

$$\frac{\partial \bar{\eta}(\omega)}{\partial x} = \varepsilon \cdot \frac{\omega^2 - 1}{2 \cdot \omega} \quad ; \quad 0 < \omega < 1 \quad (9.12)$$

10. NUMERICAL ANALYSIS

For general shape hydrofoils we compute the derived formulas in the previous sections numerically.

Whenever an integration in η from 0 to t is involved we make the transformation:

$$\eta = t \cdot \sin^2(\vartheta/2) \quad (10.1)$$

$$0 \leq \eta \leq t \quad \longleftrightarrow \quad 0 \leq \vartheta \leq \pi$$

and then we use Simpson's rule with K uniform intervals (i.e., $2 \cdot K + 1$ points).

For example equation (4.9) becomes:

$$\sigma = \frac{4 \cdot \sqrt{2} \cdot r^4}{\pi \cdot (r^2 + 1)} \cdot \int_0^\pi \frac{t \cdot \sin^2(\vartheta/2)}{(1 + t^2 \cdot \sin^4(\vartheta/2))^2} \cdot \left\{ a + b \cdot t \cdot \sin^2(\vartheta/2) \right\} \cdot \left(-\frac{\partial \bar{\eta}}{\partial x} \right) \cdot d\vartheta \quad (10.2)$$

The integrand,

$$f(\vartheta) = \frac{t \cdot \sin^2(\vartheta/2)}{(1 + t^2 \sin^4(\vartheta/2))^2} \cdot \left\{ a + b \cdot t \cdot \sin^2(\vartheta/2) \right\} \cdot \left(-\frac{\partial \bar{\eta}}{\partial x} \right) \quad (10.3)$$

behaves at the limits of the integration as follows:

at $\vartheta = 0$:

If the foil has leading edge radius ρ_L then:

$$\bar{\eta} \sim -\sqrt{2 \cdot \rho_L \cdot \xi} \quad \text{as } \xi \rightarrow 0$$

and

$$\frac{\partial \bar{\eta}}{\partial x} \sim -\sqrt{\frac{\rho_L}{2}} \cdot \frac{1}{\sqrt{\xi}} \quad (10.4)$$

or by using (3.8) and (10.1)

$$\frac{\partial \bar{\eta}}{\partial x} \sim -\sqrt{\frac{\rho_L}{2 \cdot \ell}} \cdot \frac{1}{\eta} \sim -\sqrt{\frac{\rho_L}{2 \ell}} \cdot \frac{4}{t} \cdot \frac{1}{\vartheta^2} \quad \text{as } \vartheta \rightarrow 0 \quad (10.5)$$

and

$$f(0) = a \cdot \sqrt{\frac{\rho_L}{2 \ell}} \quad (10.6)$$

at $\vartheta = \pi$: $f(\vartheta)$ is also finite as long as $\frac{\partial \bar{\eta}}{\partial x}$ is (which is the usual case).

Therefore by working in terms of ϑ we avoid the square root singularities in (4.9).

We apply the same technique for the integrals involved in the formulas (5.11), (6.9) and (8.5).

To find the shape of the cavity we numerically compute the formulas (7.1) and (8.6) by using Simpson's rule in the transformed variable ϕ : (see also Appendix C)

$$\xi = \ell \cdot \sin^2\left(\frac{\phi}{2}\right) \quad (10.7)$$

$$0 \leq \xi \leq \ell \quad \longleftrightarrow \quad 0 \leq \phi \leq \pi$$

To compute (7.1) we need to know how $\bar{q}(\bar{z})$ behaves at the leading edge ($\bar{z}=0$) and trailing edge ($\bar{z}=\infty$) of the cavity. Using formulas (6.9) we get the following asymptotic behaviors: (see Appendix B)

at $\bar{z}=0$:

$$\bar{q}(\bar{z}) = -2 \cdot \mathcal{G}^*(\bar{z}) \quad (10.8)$$

which states that the cavity for rounded nosed hydrofoils starts tangent to the upper part of the foil.

at $\bar{z}=\infty$:

$$\bar{q}(\bar{z}) \sim - \left\{ \frac{\sqrt{r^2+1}}{\sqrt{2} \cdot r^2} + \frac{2}{\pi} \cdot \int_0^{\bar{z}} \sqrt{\frac{\omega}{t-\omega}} \cdot \frac{1}{1+\omega^2} \cdot \mathcal{G}^* \cdot d\omega \right\} \cdot \bar{z} \quad (10.9)$$

which is the expected square root singularity.

The integral in (10.9) is computed numerically after making the transformation (10.1).

The sensitivity analysis of the involved numerical integrations for the special cases of a flat plate and an elliptic foil is described in Appendix C.

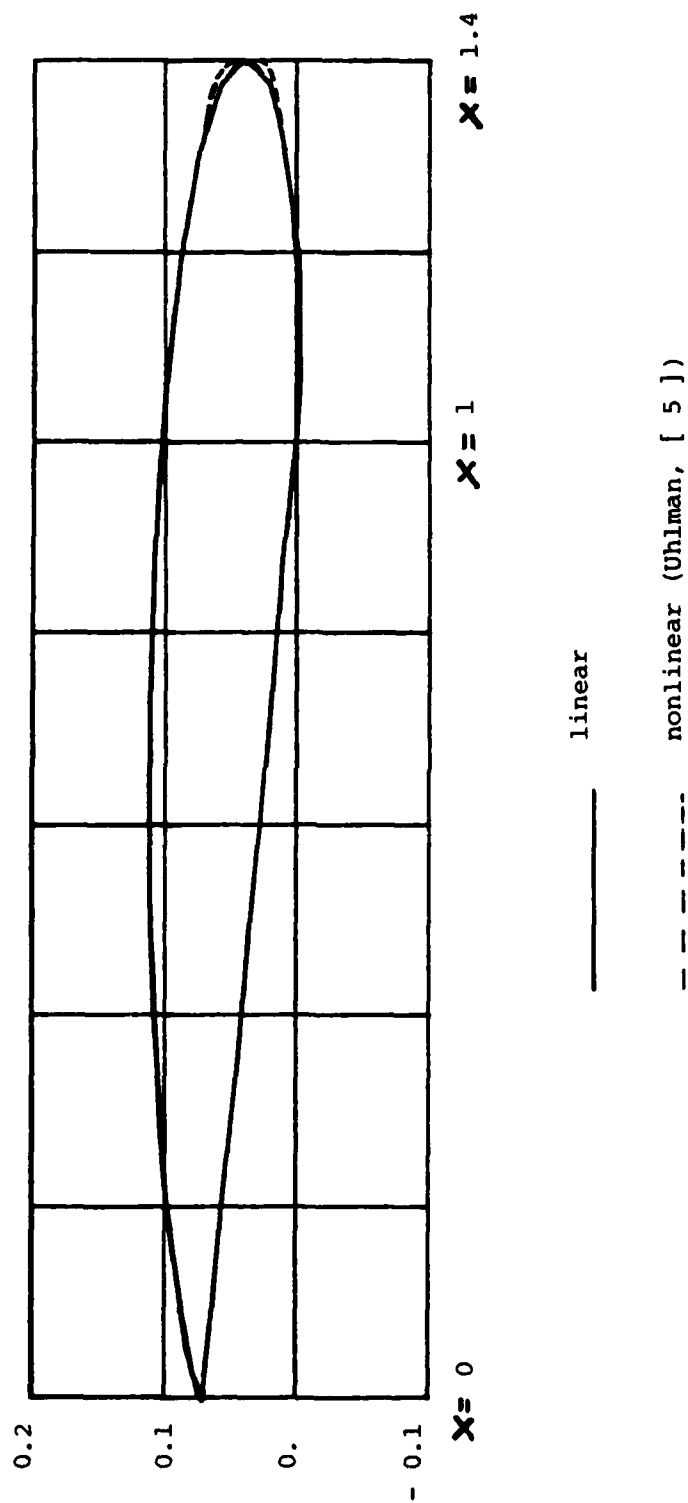
A comparison for the cavity shape of the linear to the non-linear theory as developed in [5] can be seen in Fig 5 . We observe that the two shapes are very close, except at the trailing edge of the cavity, which is due to the imposed Riboushinski model in the non-linear theory.

Finally, the analysis described above is applied to the series of NACA $a = 0.8$ meanlines and NACA 00 thickness forms for which tabulated results along with some cavity plots are included in Appendix D.

FIGURE 5

COMPARISON OF THE LINEAR TO THE NONLINEAR THEORY

FLAT PLATE AT $\alpha = 4^\circ$ ($\ell/c = 1.4$)



REFERENCES

- [1] Hanaoka, T., "Linearized Theory of Cavity Flow Past a Hydrofoil of Arbitrary Shape", Ship Research Institute, Tokyo, Japan, Paper No. 21, 1967.
- [2] Persson, B., "Theoretical Study of Cavitation on Flat Plate", DnV Technical Report 78/440.
- [3] Geurst, J.A., "Linearized Theory for Fully Cavitated Hydrofoils", International Shipbuilding Progress, Vol. 7, No. 65, Jan. 1960.
- [4] Vandyke, M. "Perturbation Methods in Fluid Mechanics", The Parabolic Press, 1975.
- [5] Uhlman, J.S., "The Surface Singularity Method Applied to Partially Cavitating Hydrofoils", Ph.D. Thesis, MIT, Department of Ocean Engineering, January 1983.
- [6] Gradshteyn, I.S. and Ryzhik, I.M., "Table of Integrals, Series, and Products", Academic Press, 1980.
- [7] Abbott, I.H. and Von Doenhoff A., "Theory of Wing Sections", Dover Publications, 1958.
- [8] Tulin, M.P., "Supercavitating Flow Past Foils and Struts", Paper No 16, Symposium on Cavitation in Hydrodynamics, September 1955, NPL, Teddington, England.
- [9] Wu, T.Y., "A Note on the Linear and Nonlinear Theories for Fully Cavitated Hydrofoils", California Institute of Technology, Hydrodynamics Laboratory Report No. 21-22, August 1956.
- [10] Parkin, B.R., "Munk Integrals for Fully Cavitated Hydrofoils", RAND Report P-2350-1, November, 1961.
- [11] Fabula, A.G., "Application of Thin-Airfoil Theory to Hydrofoils with Cut-off Ventilated Trailing Edge", Navveps Report 7571 NOTS TP 2547, U.S. Naval Ordnance Test Station China Lake, California, September 13, 1960.
- [12] Fabula, A.G., "Thin-Airfoil Theory Applied to Hydrofoils With a Single Finite Cavity and Arbitrary Free-Streamline Detachment", JFM, Vol. 12, 1962, pp. 227-240.

APPENDIX A

LIST OF INTEGRALS

In this Appendix, a list of integrals used throughout our analysis is given, along with instructions for their derivation.

The first integrals (A.1) - (A.9) have been taken from Appendix A of

[2]

$$r^4 = 1 + t^2, \quad t^2 = 1/(e-1)$$

$$\int_0^t \sqrt{\frac{z}{t-z}} \cdot \frac{1}{1+z^2} \cdot dz = \frac{\pi}{\sqrt{2}} \cdot \frac{\sqrt{r^2-1}}{r^2} \quad (\text{A.1})$$

$$\int_0^t \sqrt{\frac{z}{t-z}} \cdot \frac{z}{1+z^2} \cdot dz = \pi - \frac{\pi}{\sqrt{2}} \cdot \frac{\sqrt{r^2+1}}{r^2} \quad (\text{A.2})$$

$$\int_0^t \sqrt{\frac{z}{t-z}} \cdot \frac{z^2}{1+z^2} \cdot dz = \frac{\pi \cdot t}{2} - \frac{\pi}{\sqrt{2}} \cdot \frac{\sqrt{r^2-1}}{r^2} \quad (\text{A.3})$$

$$\int_0^t \sqrt{\frac{z}{t-z}} \cdot \frac{1}{(1+z^2)^2} \cdot dz = \frac{\pi}{4\sqrt{2}} \cdot \frac{t(t^2+3) \cdot \sqrt{r^2+1} - 2 \cdot \sqrt{r^2-1}}{r^8} \quad (\text{A.4})$$

$$\int_0^t \sqrt{\frac{z}{t-z}} \cdot \frac{z}{(1+z^2)^2} \cdot dz = \frac{\pi}{4\sqrt{2}} \cdot \frac{2t^2 \cdot \sqrt{r^2+1} + t \cdot (t^2-1) \cdot \sqrt{r^2-1}}{r^8} \quad (\text{A.5})$$

$$\int_0^t \sqrt{\frac{z}{t-z}} \cdot \frac{z^2}{(1+z^2)^2} \cdot dz = \frac{\pi}{4\sqrt{2}} \cdot \frac{t(3t^2+1) \cdot \sqrt{r^2+1} - (4t^2+2) \cdot \sqrt{r^2-1}}{r^8} \quad (\text{A.6})$$

$$\int_0^t \sqrt{\frac{t-z}{z}} \cdot \frac{1}{1+z^2} \cdot dz = \frac{\pi}{\sqrt{2}} \cdot \sqrt{r^2-1} \quad (\text{A.7})$$

$$\int_0^t \sqrt{\frac{t-z}{z}} \cdot \frac{z}{1+z^2} \cdot dz = \frac{\pi}{\sqrt{2}} \cdot \sqrt{r^2+1} - \pi \quad (\text{A.8})$$

$$\int_0^t \sqrt{\frac{t-z}{z}} \cdot \frac{z^2}{1+z^2} \cdot dz = \frac{\pi \cdot t}{2} - \frac{\pi}{\sqrt{2}} \cdot \sqrt{r^2-1} \quad (\text{A.9})$$

The next integrals (A.10) - (A.16) are computed by using the transformation $x = \ell \cdot \sin^2\left(\frac{\vartheta}{2}\right)$ or $z = t \cdot \sin^2\left(\frac{\vartheta}{2}\right)$; $0 \leq \vartheta \leq \pi$ (see also [6])

$$\int_0^{\ell} \sqrt{\frac{x}{\ell-x}} \cdot dx = \frac{\pi \cdot \ell}{2} \quad (\text{A.10})$$

$$\int_0^{\ell} x \cdot \sqrt{\frac{x}{\ell-x}} \cdot dx = \frac{3\pi \ell^2}{8} \quad (\text{A.11})$$

$$\int_0^{\ell} x \cdot \sqrt{\frac{x}{\ell-x}} \cdot \frac{1}{x-\xi} \cdot dx = \pi \cdot \left(\xi + \frac{\ell}{2}\right); \quad 0 \leq \xi \leq \ell \quad (\text{A.12})$$

$$\int_0^t \sqrt{\frac{z}{t-z}} \cdot \frac{1}{\eta-z} \cdot dz = -\pi \quad ; \quad 0 \leq \eta \leq t \quad (\text{A.13a})$$

$$= \pi \cdot \sqrt{\frac{\eta}{\eta-t}} - \pi \quad ; \quad \eta > t \quad (\text{A.13b})$$

$$\int_0^t \sqrt{\frac{t-z}{z}} \cdot \frac{1}{\eta-z} \cdot dz = \pi \quad ; \quad 0 \leq \eta \leq t \quad (\text{A.14a})$$

$$= \pi - \pi \cdot \sqrt{\frac{\eta-t}{\eta}} \quad ; \quad \eta > t \quad (\text{A.14b})$$

$$\int_0^t \sqrt{\frac{t-z}{z}} \cdot \frac{1}{\eta+z} \cdot dz = \pi \cdot \sqrt{\frac{\eta+t}{\eta}} - \pi \quad ; \quad z > 0 \quad (\text{A.15})$$

$$\int_0^t \sqrt{\frac{z}{t-z}} \cdot \frac{1}{\eta+z} \cdot dz = \pi - \pi \cdot \sqrt{\frac{\eta}{\eta+t}} \quad ; \quad z > 0 \quad (\text{A.16})$$

The next integrals are reduced into a linear combination of the previous integrals as follows:

$$\text{a) } I(\eta) = \int_0^t \sqrt{\frac{t-z}{z}} \cdot \frac{1}{1+z^2} \cdot \frac{1}{z-\eta} \cdot dz \quad ; \quad 0 \leq \eta \leq t$$

We break the integrand into simpler fractions:

$$\bar{\eta}(x) = -0.5 \cdot (0.29690 \cdot \sqrt{x} - 0.12600 \cdot x - 0.35160 \cdot x^2 + 0.28430 \cdot x^3 - 0.10150 \cdot x^4), \quad (D.3)$$

for $0 < x < 1$

The results for σ and V_{c2} are given in Tables 9 and 10 (see also Figures 10 and 11) along with some cavity plots in Figures 7a, 7b, 7c, 8a, 8b, 8c. The values for σ and V_{c2} have been computed with $K = 50$ in order to get the first five decimal places correct (although we get the same accuracy with much smaller K for larger l/c) and the cavity plots have been made with $K = 30$ points (although the cavity shape has been found very insensitive to K for a broad range of l/c). Most of the plots have no physical meaning but if combined with the appropriate angle of attack so that the cavity clears off the upper part of the hydrofoil then they give meaningful solutions to our problem.

In case our hydrofoil consists of a NACA $a = 0.8$ meanline of maximum camber f_{max} , a NACA 00 thickness form of maximum thickness t_{max} , and operates at an angle of attack α , then according to Section 2, any quantity Q can be expressed as: (keeping always the same cavity length)

$$Q = \frac{f_{max}}{0.0679 \cdot c} \cdot Q_{0.8} + \frac{t_{max}}{0.1 \cdot c} \cdot Q_{0010} + \frac{\left[\alpha - \alpha_c \frac{f_{max}}{0.0679 \cdot c} \right]^2}{4^2} \cdot Q_4 \quad (D.4)$$

where:

$$Q_{0.8} : Q \text{ for NACA } a = 0.8, f_{max}/c = 0.0679$$

$$Q_{0010} : Q \text{ for NACA 0010}$$

APPENDIX D

SUPERCAVITATING NACA $a = 0.8$ MEANLINES AND NACA 00 THICKNESS FORMS

The analysis described in the previous sections has been carried out for a NACA $a = 0.8$ meanline (with $t_{max}/c = 0.0679$) and a NACA 0010 thickness form.

For the NACA $a = 0.8$ at $\alpha = \alpha_i$; we put as $\bar{\eta}(x)$ the analytical expression from [7]:

$$\begin{aligned} \bar{\eta}(x) = \frac{C_{Li}}{2\pi(a+1)} \cdot \left\{ \frac{1}{1-\alpha} \cdot \left[\frac{1}{2} \cdot (\alpha-x)^2 \cdot \ln|\alpha-x| - \right. \right. \\ \left. \left. - \frac{1}{2} \cdot (1-x)^2 \cdot \ln(1-x) + \frac{1}{4} \cdot (1-x)^2 - \frac{1}{4} (\alpha-x)^2 \right] - \right. \\ \left. - x \cdot \ln x + g - h \cdot x \right\} + (1-x) \cdot \alpha_i, \end{aligned} \quad (D.1)$$

for $0 < x < 1$

where:

$$\begin{aligned} a = 0.8, \quad C_{Li} = 1, \quad \alpha_i = 1.54^\circ \\ g = -0.009297, \quad h = -0.3039 \end{aligned} \quad (D.2)$$

For the NACA 0010 thickness form at $\alpha = 0^\circ$ we also take from [7]:

ELLIPTIC FOIL AT $\ell/c = 2$ ($\epsilon = 1$)

Table 7

CAVITY THICKNESSES h_i 's ($K = 20$)			
i	x/c	Numerical	Analytical
1	0.000000	0.000000	0.000000
2	0.012312	0.312869	0.312869
3	0.048942	0.618034	0.618034
4	0.108993	0.907981	0.907981
5	0.190983	1.175571	1.175571
6	0.292003	1.414214	1.414214
7	0.412210	1.618034	1.618034
8	0.546010	1.782013	1.782013
9	0.690983	1.902113	1.902113
10	0.843566	1.975377	1.975377
11	1.000000	2.000000	2.000000
12	1.156424	1.975377	1.975377
13	1.309017	1.902113	1.902113
14	1.453990	1.782013	1.782013
15	1.597785	1.618034	1.618034
16	1.727107	1.414214	1.414214
17	1.839017	1.175571	1.175571
18	1.921067	0.907981	0.907981
19	1.951057	0.618034	0.618034
20	1.921069	0.312869	0.312869
21	2.000000	-0.000000	0.000000

ELLIPTIC FOIL AT $\frac{b}{c} = 2$ ($\epsilon = 1$)

Table 6

CAVITY THICKNESSES h_i 's ($K = 5$)			
i	x/c	Numerical	Analytical
1	0.000000	0.000000	0.000000
2	0.100993	1.175635	1.175571
3	0.600993	1.902217	1.902113
4	1.000017	1.902217	1.902113
5	1.000017	1.175635	1.175571
6	2.000000	-0.000000	0.000000
CAVITY THICKNESSES h_i 's ($K = 10$)			
1	0.000000	0.000000	0.000000
2	0.048943	0.618036	0.618034
3	0.190903	1.175574	1.175571
4	0.412215	1.618039	1.618034
5	0.690993	1.902119	1.902113
6	1.000000	2.000007	2.000000
7	1.000017	1.902119	1.902113
8	1.500000	1.618039	1.618034
9	1.900017	1.175574	1.175571
10	1.951057	0.618036	0.618034
11	2.000000	0.000000	0.000000

ELLIPTIC FOIL AT $b/c = 2$ ($\epsilon = 1$)

Table 4

	σ	V/c^2
Analytical	2.	3.14159265
$K = 20$	2.00000000	3.14159265
$K = 10$	2.00000000	3.14159265
$K = 5$	1.99999994	3.14159217
$K = 3$	1.99866994	3.13764913

Table 5

CAVITY SOURCE DISTRIBUTION $\bar{q}(x)$				
x/c	Analytical	Numerical		
		$K = 20$	$K = 10$	$K = 3$
0.1	2.06474	2.06474	2.06474	2.06206
0.2	1.33333	1.33333	1.33333	1.33270
0.4	0.75000	0.75000	0.75000	0.74987
0.5	0.57735	0.57735	0.57735	0.57727
0.7	0.31449	0.31449	0.31449	0.31444
0.9	0.10050	0.10050	0.10050	0.10046
1.	0.	0.00000	0.00000	- 0.00005

FLAT PLATE AT $l/c = 1.4$, $\alpha = 1$ rad

Table 3

CAVITY SOURCE DISTRIBUTION $\bar{q}(x)$		
x/c	Analytical	Numerical
0.10000000D-02	0.28948538D+01	0.28948538D+01
0.10000000D-01	0.16006528D+01	0.16006528D+01
0.10000000D+00	0.83092970D+00	0.83092969D+00
0.30000000D+00	0.54165536D+00	0.54165536D+00
0.50000000D+00	0.39457754D+00	0.39457754D+00
0.80000000D+00	0.21229725D+00	0.21229725D+00
0.10000000D+01	0.69210140D-01	0.69210140D-01
0.12000000D+01	-0.69955753D+00	-0.69955753D+00
0.13500000D+01	-0.20259790D+01	-0.20259790D+01
0.13990000D+01	-0.15589989D+02	-0.15589989D+02

FLAT PLATE AT $\alpha = 1$ rad

Table 1

CAVITATION NUMBER σ				
l/c	Analytical	Numerical		
		$K = 20$	$K = 10$	$K = 5$
1.1	6.324555	6.324555	6.324560	6.329471
1.3	3.651484	3.651484	3.651484	3.651730
1.5	2.828427	2.828427	2.828427	2.828405
1.8	2.236068	2.236068	2.236068	2.236057
2.0	2.	2.000000	2.000000	1.999995

Table 2

CAVITY VOLUME V/c^2				
l/c	Analytical	Numerical		
		$K = 20$	$K = 10$	$K = 5$
1.1	1.272656	1.272656	1.272668	1.282604
1.3	1.327715	1.327715	1.327715	1.328218
1.5	1.554475	1.554475	1.554475	1.554295
1.8	1.975729	1.975729	1.975729	1.975635
2.0	2.288818	2.288818	2.288818	2.288768

For a supercavitating flat plate at $\alpha = 4^\circ$ and different cavity lengths, the values for σ and $\sqrt{V/c^2}$ are given in Table 8 (see also Figures 10 and 11), and some cavity plots are shown in Figures 6a, 6b, 6c.

APPENDIX C

CONVERGENCE OF THE NUMERICAL INTEGRATIONS

The numerical analysis as described in Section 10 has been tried for the special cases of a flat plate (Tables 1 and 2) and an elliptic foil (Tables 4-7) for which the analytical results are given in Section 9. The results are very good even for small K .

For the computation of the cavity source distribution $\bar{q}(x)$ for a flat plate $K = 50$ has been used for $0 < x < 0.1$ and $1 < x < 1.2$, and $K = 10$ elsewhere, to give us the excellent results as shown in Table 3.

The cavity thicknesses have been computed using (7.1) and the transformation (10.7) as follows:

$$h_{i+1} = h_i + \sigma \cdot \int_{\phi_i}^{\phi_{i+1}} \bar{q}(x) \cdot \frac{dx}{d\phi} \cdot d\phi \quad ; \quad i=1, K \quad (C.1)$$

$$h_1 = 0 \quad (C.2)$$

$$\phi_{i+1} = \phi_i + \pi/K \quad (C.3)$$

The integral in C.1 has been evaluated by using Simpson's rule in one interval between ϕ_i and ϕ_{i+1} . A check to our numerical integrations should be the closure condition:

$$h_{K+1} = 0 \quad (C.4)$$

A similar (if not better) convergence is found for the camber distribution $C(x)$ in the wake of the cavity.

$$\bar{q}(z) \sim \left\{ -\frac{\sqrt{r^2+1}}{\sqrt{2} \cdot r^2} - \frac{2}{\pi} \cdot \int_0^+ \sqrt{\frac{\omega}{z-\omega}} \cdot \frac{1}{1+\omega^2} \cdot g^*(\omega) \cdot d\omega \right\} \cdot z \quad (\text{B.10})$$

as $z \rightarrow \infty$ and for both, either sharp or rounded nosed hydrofoils.

$$F(z) = \int_0^t \sqrt{\frac{\omega}{t-\omega}} \cdot \frac{1}{1+\omega^2} \cdot \frac{\vartheta^*(\omega)}{z+\omega} \cdot d\omega \quad (B.5)$$

Since now $\vartheta^*(\omega) \sim -\frac{G}{\omega}$ as $\omega \rightarrow 0$ then $\sqrt{\frac{\omega}{t-\omega}} \cdot \frac{1}{1+\omega^2} \cdot \vartheta^*(\omega) \sim -\frac{G}{\sqrt{t} \cdot \sqrt{\omega}}$

as $\omega \rightarrow 0$ and $F(z) \sim F_0(z)$ as $z \rightarrow 0$, where:

$$F_0(z) = -\frac{G}{\sqrt{t}} \cdot \int_0^t \frac{d\omega}{\sqrt{\omega} \cdot (z+\omega)} = -\frac{2.G}{\sqrt{t} \cdot \sqrt{z}} \cdot \arctan\left(\frac{\sqrt{t}}{\sqrt{z}}\right) \quad (B.6)$$

But:

$$F_0(z) \sim -\frac{2.G}{\sqrt{t} \cdot \sqrt{z}} \cdot \frac{\pi}{2} = -\frac{\pi.G}{\sqrt{t} \cdot \sqrt{z}} \quad \text{as } z \rightarrow 0$$

Thus:

$$F(z) \sim -\frac{\pi.G}{\sqrt{t} \cdot \sqrt{z}} \quad \text{as } z \rightarrow 0 \quad (B.7)$$

and finally $\bar{q}(z) \sim -\frac{2.G}{z}$ or:

$$\bar{q}(z) \sim -2 \cdot \vartheta^*(z) \quad \text{as } z \rightarrow 0, \quad (B.8)$$

which means that for round nosed hydrofoils the cavity has the same slope and curvature with the wetted part of the hydrofoil at the leading edge.

b) Sharp nosed hydrofoils

The asymptotic behavior of $\bar{q}(z)$ will be: (as $z \rightarrow 0$)

$$\bar{q}(z) \sim \left\{ \frac{t^{1/2} \cdot \sqrt{r^2-1}}{2 \cdot \sqrt{z} \cdot r^2} - \frac{t^{1/2}}{\pi} \cdot \int_0^t \frac{1}{\sqrt{\omega} \cdot (t-\omega)} \cdot \frac{1}{1+\omega^2} \cdot \vartheta^*(\omega) \cdot d\omega \right\} \frac{1}{\sqrt{z}} \quad (B.9)$$

since $\vartheta^*(z) < \frac{1}{\sqrt{z}}$ as $z \rightarrow 0$ (even for NACA a = 0.8 meanline)

Now at the trailing edge of the cavity ($z = \infty$ or $x = \ell$)

by using (6.9b) we get the asymptotic behavior of $\bar{q}(z)$ as:

APPENDIX B

ASYMPTOTIC BEHAVIOR OF $\bar{\eta}(z)$ AT THE LEADING AND TRAILING EDGES OF THE CAVITY

First, at the leading edge of the cavity and foil
($z = 0$ or $x = 0$) we consider the following cases:

a) Round nosed hydrofoils

If the leading edge radius is ρ_L we have

$$\bar{\eta} \sim -\sqrt{2 \cdot \rho_L \cdot x} \quad \text{as} \quad x \rightarrow 0 \quad (\text{B.1})$$

and by using (3.1) we get:

$$\vartheta^*(x) = \frac{1}{\sigma} \cdot \frac{\partial \bar{\eta}}{\partial x} = -\frac{1}{\sigma} \cdot \sqrt{\frac{\rho_L}{2}} \cdot \frac{1}{\sqrt{x}} \quad \text{as} \quad x \rightarrow 0 \quad (\text{B.2})$$

But $z \sim \frac{\sqrt{x}}{\sqrt{\ell}}$ as $x \rightarrow 0$, according to (3.8)

Thus

$$\vartheta^*(z) \sim -\frac{G}{z} \quad \text{as} \quad z \rightarrow 0 \quad (\text{B.3})$$

with

$$G = \frac{1}{\sigma} \cdot \sqrt{\frac{\rho_L}{2 \cdot \ell}} \quad (\text{B.4})$$

To find the asymptotic behavior of (6.9a) as $z \rightarrow 0$ we need first to
work on the integral:

$$\frac{1}{(z^2 - \eta^2) \cdot (\eta - \omega)} = \frac{A}{z - \eta} + \frac{B}{z + \eta} + \frac{C}{\eta - \omega}$$

with:

$$A = \frac{1}{2z \cdot (z - \omega)} \quad , \quad B = -\frac{1}{2z \cdot (z + \omega)} \quad , \quad C = \frac{\omega}{z \cdot (z^2 - \omega^2)}$$

and finally we get:

$$R(\omega, z) = -\frac{\pi}{2z(z+\omega)} \cdot \sqrt{\frac{t+z}{z}} \quad ; \quad 0 \leq z \leq t \quad (\text{A.19a})$$

$$R(\omega, z) = -\frac{\pi}{2z(z+\omega)} \cdot \sqrt{\frac{t+z}{z}} - \frac{\pi}{2z(z-\omega)} \cdot \sqrt{\frac{z-t}{z}} \quad ; \quad z > t \quad (\text{A.19b})$$

Similarly as in the previous sections we can derive:

$$\begin{aligned} S(z) &= \int_0^t \sqrt{\frac{\omega}{t-\omega}} \cdot \frac{1}{1+\omega^2} \cdot \frac{\omega}{z+\omega} \cdot d\omega = \\ &= \frac{1}{1+z^2} \cdot \frac{\pi}{12 \cdot r^2} \cdot \left[\sqrt{r^2+1} - z \cdot \sqrt{r^2+1} \right] + \pi \cdot \sqrt{\frac{z}{z+t}} \cdot \frac{z}{1+z^2} \quad ; \quad z > 0 \quad (\text{A.20}) \end{aligned}$$

$$\begin{aligned} P(z) &= \int_0^t \sqrt{\frac{\omega}{t-\omega}} \cdot \frac{1}{1+\omega^2} \cdot \frac{\omega}{z-\omega} \cdot d\omega = \\ &= -\frac{1}{1+z^2} \cdot \frac{\pi}{12 \cdot r^2} \cdot \left[\sqrt{r^2+1} z + \sqrt{r^2+1} \right] + \pi \cdot \sqrt{\frac{z}{z-t}} \cdot \frac{z}{1+z^2} \quad ; \quad z > t \quad (\text{A.21}) \end{aligned}$$

$$\begin{aligned} B(\omega, z) &= \int_0^t \sqrt{\frac{t-\eta}{\eta}} \cdot \frac{\eta}{(z^2 - \eta^2) \cdot (\eta - \omega)} \cdot d\eta = \\ &= \frac{\pi}{z} \cdot \left[\frac{1}{z+\omega} \cdot \sqrt{\frac{t+z}{z}} - \frac{1}{z-\omega} \cdot \sqrt{\frac{z-t}{z}} \right] \quad ; \quad z \geq t \quad (\text{A.22}) \end{aligned}$$

$$\frac{1}{1+z^2} \cdot \frac{1}{z-\eta} = \frac{Az+B}{1+z^2} + \frac{C}{z-\eta}$$

where:

$$A = -\frac{1}{1+\eta^2}, \quad B = -\frac{\eta}{1+\eta^2}, \quad C = \frac{1}{1+\eta^2}$$

and finally by plugging in the known integrals we get:

$$I(\eta) = -\frac{\pi}{\sqrt{2} \cdot (1+\eta^2)} \cdot (\alpha + b \cdot \eta) \quad (\text{A.17})$$

$$\text{where: } \alpha = \sqrt{r^2+1}, \quad b = \sqrt{r^2-1}$$

$$\begin{aligned} \text{b) } J(\eta) &= \int_0^t \frac{z^2}{(1+z^2)^2} \cdot \sqrt{\frac{t-z}{z}} \cdot \frac{1}{z-\eta} \cdot dz = \\ &= \int_0^t \sqrt{\frac{z}{t-z}} \cdot \frac{z \cdot (t-z)}{(1+z^2)^2 \cdot (z-\eta)} \cdot dz \quad ; \quad 0 \leq \eta \leq t \end{aligned}$$

Similarly, we break the integrand:

$$\frac{z \cdot (t-z)}{(1+z^2)^2 \cdot (z-\eta)} = \frac{A \cdot z + B}{1+z^2} + \frac{C \cdot z + D}{(1+z^2)^2} + \frac{E}{z-\eta}$$

where:

$$A = \frac{\eta \cdot (\eta - t)}{(1+\eta^2)^2}, \quad B = \frac{\eta^2 \cdot (\eta - t)}{(1+\eta^2)^2}, \quad C = -\frac{1+\eta t}{1+\eta^2},$$

$$D = -\frac{(\eta - t)}{1+\eta^2}, \quad E = -\frac{\eta(\eta - t)}{(1+\eta^2)^2}$$

and finally:

$$\begin{aligned} J(\eta) &= \frac{\pi}{\sqrt{2} \cdot r^2} \cdot \frac{1}{(1+\eta^2)} \cdot \left[\frac{\eta \cdot (t-\eta)}{(1+\eta^2)} \cdot \left\{ \sqrt{r^2+1} - \eta \cdot \sqrt{r^2-1} \right\} - \right. \\ &\quad - \frac{(1+\eta \cdot t)}{4 \cdot r^6} \cdot \left\{ 2 \cdot t^2 \cdot \sqrt{r^2+1} + t \cdot (t^2-1) \cdot \sqrt{r^2-1} \right\} + \\ &\quad \left. + \frac{(t-\eta)}{4 \cdot r^6} \cdot \left\{ t \cdot (t^2+3) \cdot \sqrt{r^2+1} - 2 \cdot \sqrt{r^2-1} \right\} \right] \quad (\text{A.18}) \end{aligned}$$

$$\text{c) } R(\omega, z) = \int_0^t \sqrt{\frac{t-\eta}{\eta}} \cdot \frac{1}{z^2-\eta^2} \cdot \frac{1}{\eta-\omega} \cdot d\eta \quad ; \quad 0 \leq \omega \leq t, \quad z > 0$$

We have:

Q_{4° : Q for flat plate at angle of attack

$$\alpha = 4^\circ$$

$\alpha_i = 1.54^\circ$: ideal angle of attack for

$$\text{NACA } a = 0.8 \left(\frac{f_{max}}{c} = 0.0679 \right)$$

For example, if our hydrofoil is a combination of a NACA $a = 0.8$ meanline with $f_{max}/c = 0.0679$ and a NACA 0010 thickness distribution and operates at an angle of attack $\alpha = 7^\circ$ then:

$$\sigma = \sigma_{0.8} + \sigma_{0010} + \frac{7 - 1.54}{4} \cdot \sigma_{4^\circ} \quad (\text{D.5})$$

$$V = V_{0.8} + V_{0010} + \frac{7 - 1.54}{4} V_{4^\circ} \quad (\text{D.6})$$

If $l/c = 1.4$ then by substituting in (D.5) and (D.6) the appropriate values from Tables 8, 9 and 10 we get:

$$\sigma = 0.52946 \quad \text{and} \quad V = 0.21782 \quad (\text{D.7})$$

Also for the cavity thicknesses we will have:

$$h(x) = h_{0.8}(x) + h_{0010}(x) + \frac{7 - 1.54}{4} \cdot h_{4^\circ}(x) \quad (\text{D.8})$$

which is illustrated in Figure 9.

FLAT PLATE AT $\alpha = 4^\circ$

Table 8

l/c	σ	V/c^2
1.050	0.62443	0.10030
1.100	0.44154	0.08885
1.150	0.36051	0.08672
1.200	0.31221	0.08753
1.250	0.27925	0.08972
1.300	0.25492	0.09269
1.350	0.23601	0.09618
1.400	0.22077	0.10003
1.450	0.20814	0.10417
1.500	0.19746	0.10852
1.550	0.18827	0.11307
1.600	0.18026	0.11778
1.650	0.17319	0.12263
1.700	0.16689	0.12761
1.750	0.16123	0.13272
1.800	0.15611	0.13793
1.850	0.15145	0.14325
1.900	0.14718	0.14867
1.950	0.14325	0.15418
2.000	0.13963	0.15979

NACA $a = 0.8$ ($h_{max}/c = 0.0679$) at $\alpha = \alpha_i$

Table 9

l/c	σ	V/c^2
1.050	0.39990	-0.00494
1.100	0.32652	-0.00950
1.150	0.28970	-0.01045
1.200	0.26552	-0.01005
1.250	0.24774	-0.00886
1.300	0.23373	-0.00715
1.350	0.22226	-0.00503
1.400	0.21258	-0.00257
1.450	0.20422	0.00017
1.500	0.19688	0.00316
1.550	0.19037	0.00638
1.600	0.18453	0.00981
1.650	0.17925	0.01344
1.700	0.17441	0.01725
1.750	0.17001	0.02124
1.800	0.16594	0.02540
1.850	0.16215	0.02971
1.900	0.15864	0.03419
1.950	0.15534	0.03879
2.000	0.15226	0.04355

Table 10

l/c	σ	V/c^2
1.050	0.17643	0.08551
1.100	0.09639	0.08048
1.150	0.06359	0.07962
1.200	0.04540	0.07992
1.250	0.03381	0.08068
1.300	0.02580	0.08166
1.350	0.01996	0.08273
1.400	0.01553	0.08385
1.450	0.01207	0.08498
1.500	0.00932	0.08610
1.550	0.00708	0.08721
1.600	0.00523	0.08829
1.650	0.00369	0.08935
1.700	0.00239	0.09038
1.750	0.00128	0.09138
1.800	0.00033	0.09234
1.850	-0.00048	0.09328
1.900	-0.00120	0.09418
1.950	-0.00182	0.09505
2.000	-0.00236	0.09590

FIGURE 6a

FLAT PLATE AT $\alpha = 4^\circ$

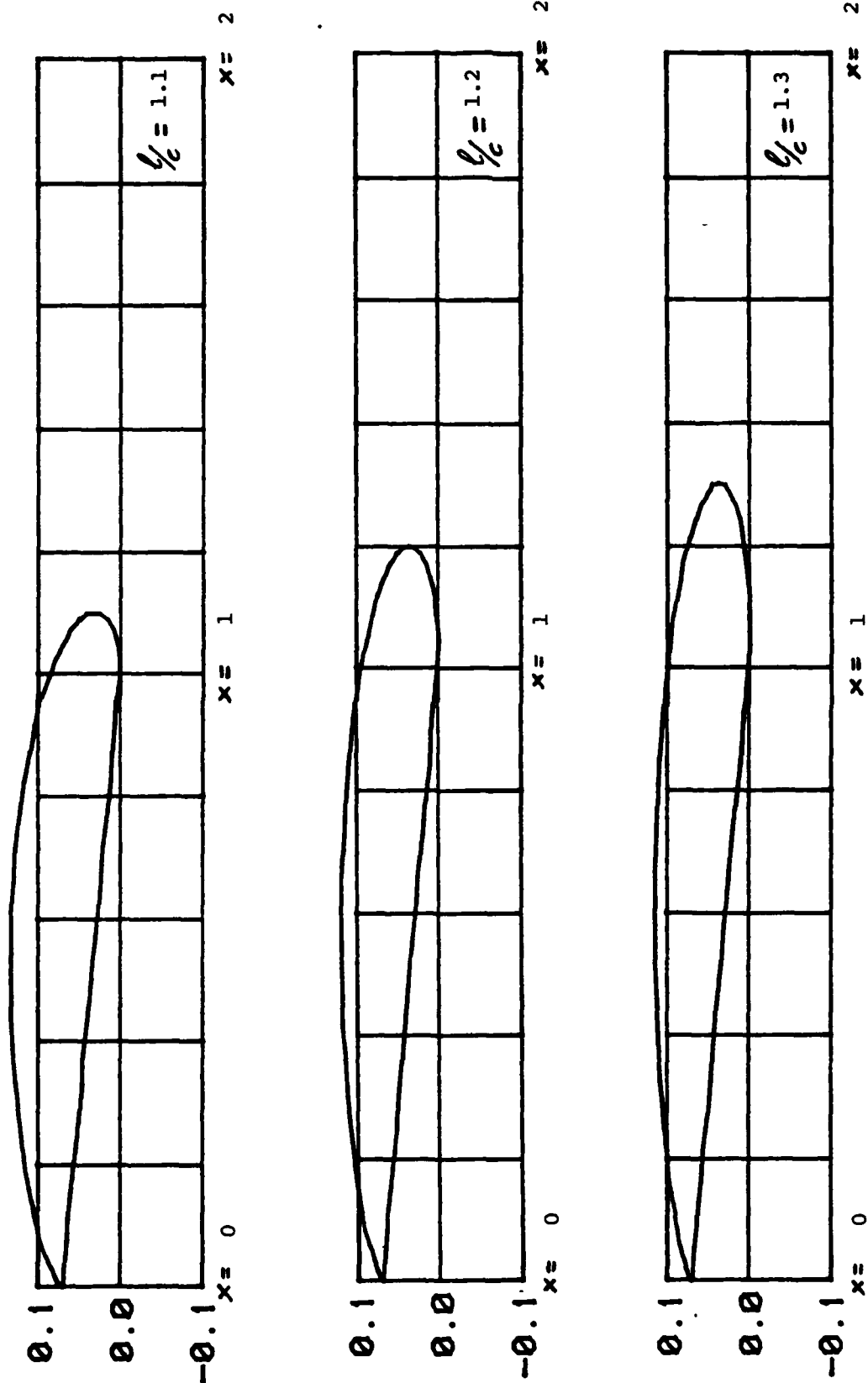


FIGURE 6b

FLAT PLATE AT $\alpha = 4^\circ$

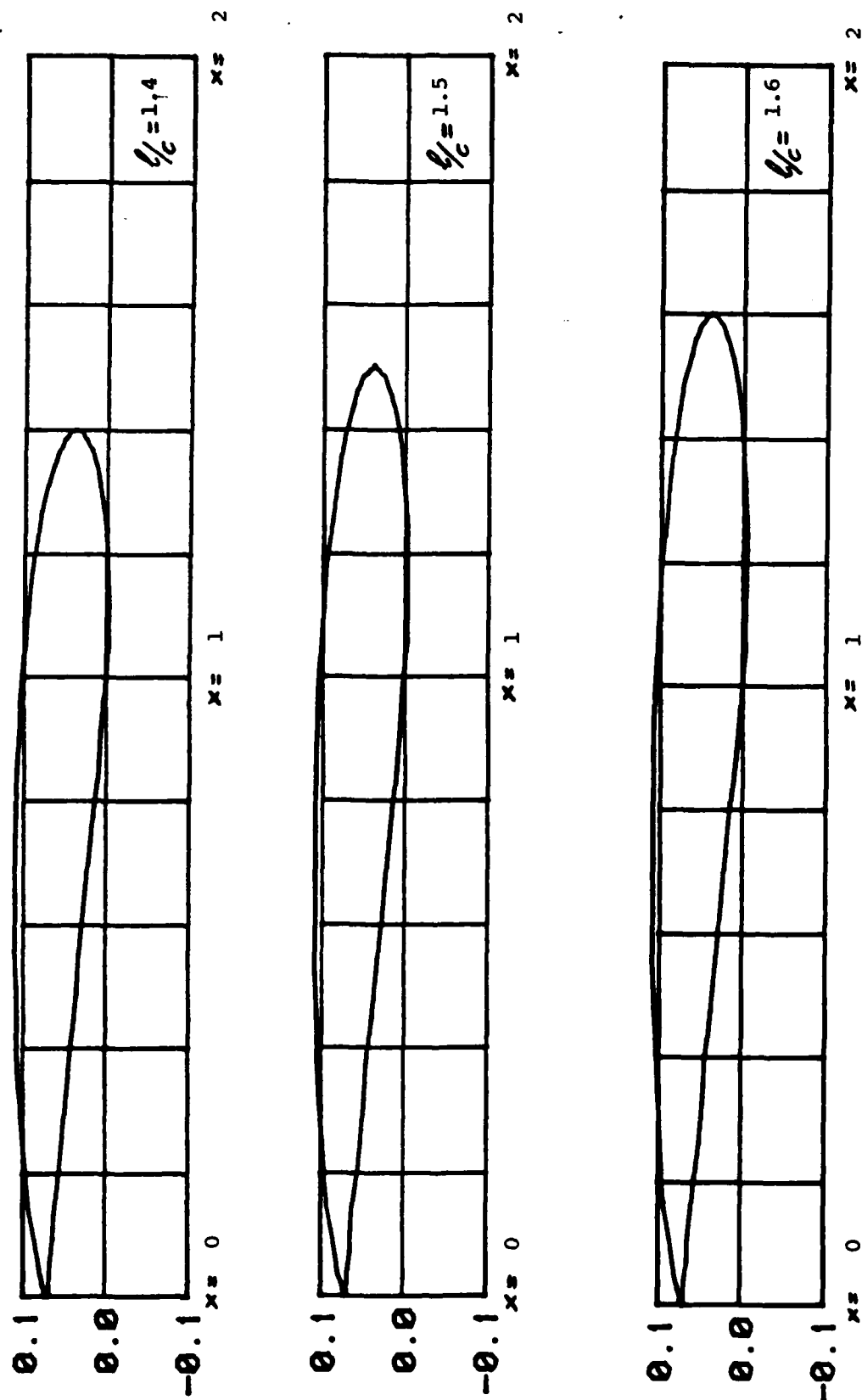


FIGURE 6c

FLAT PLATE AT $\alpha = 4^\circ$

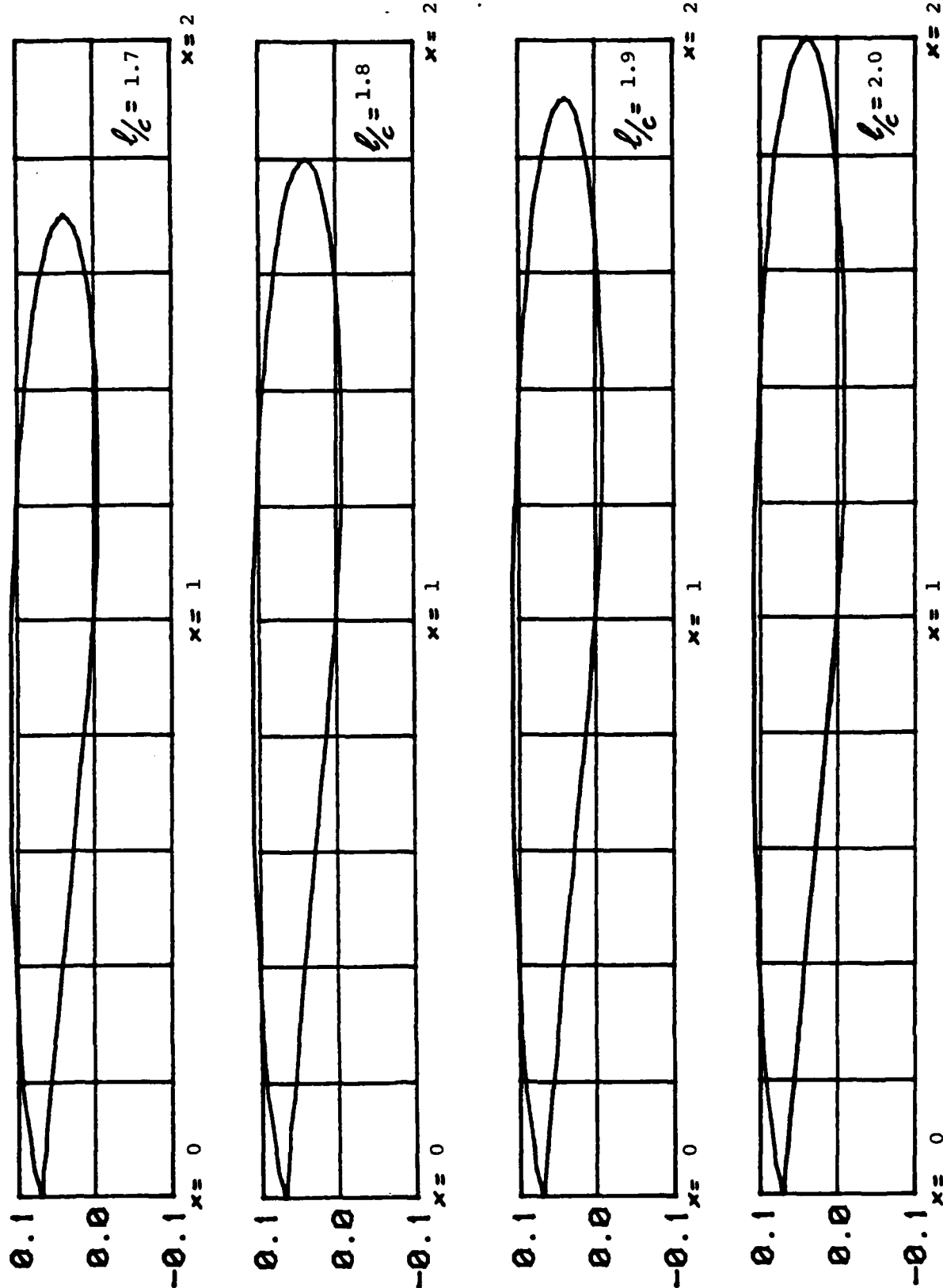


FIGURE 7a

NACA $a = 0.8$ ($h_{max}/c = 0.0679$) at $\alpha = \alpha_L$

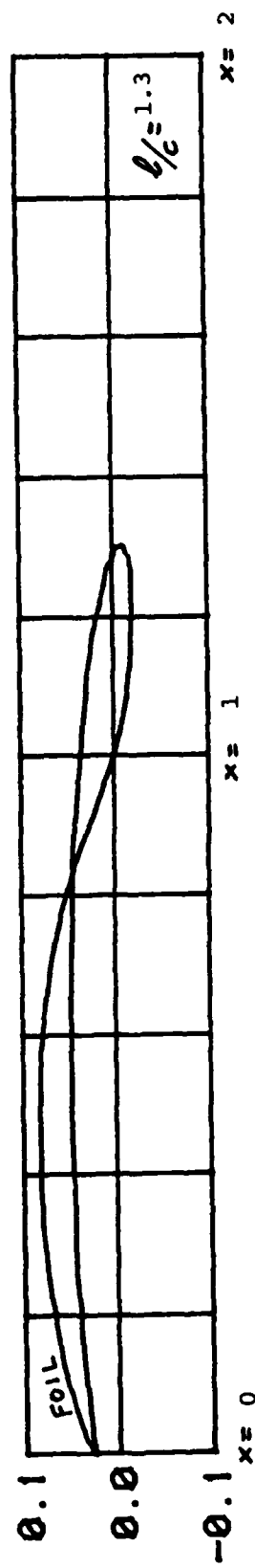
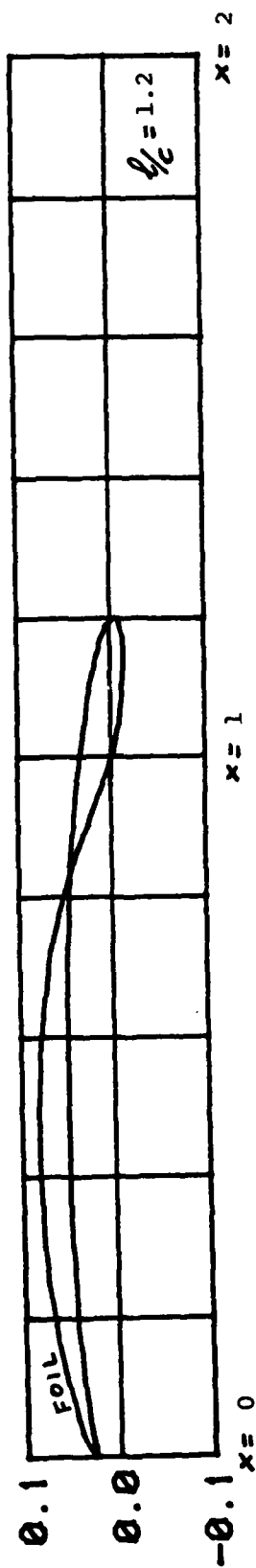
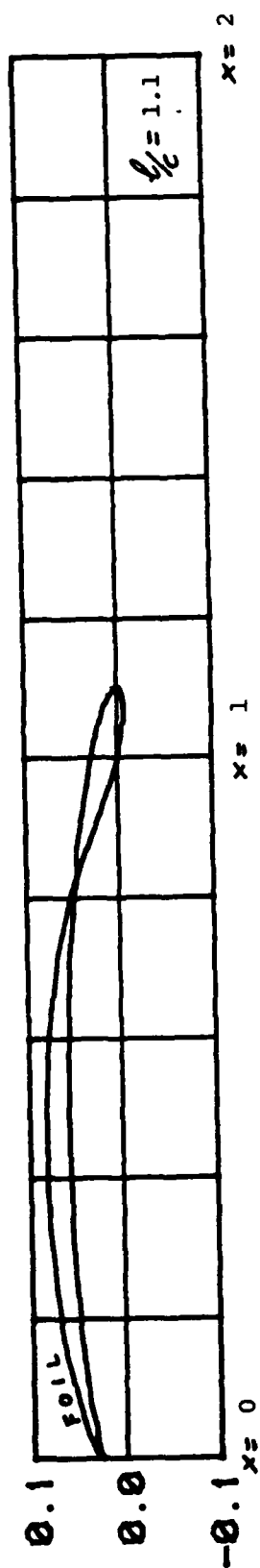
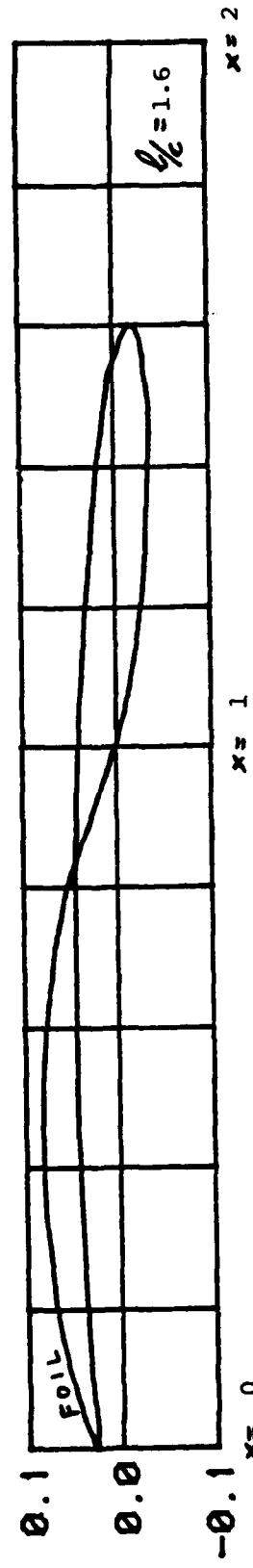
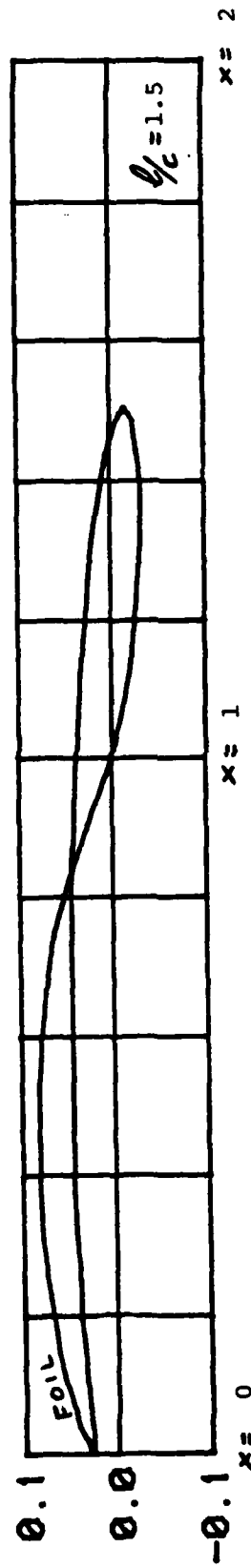
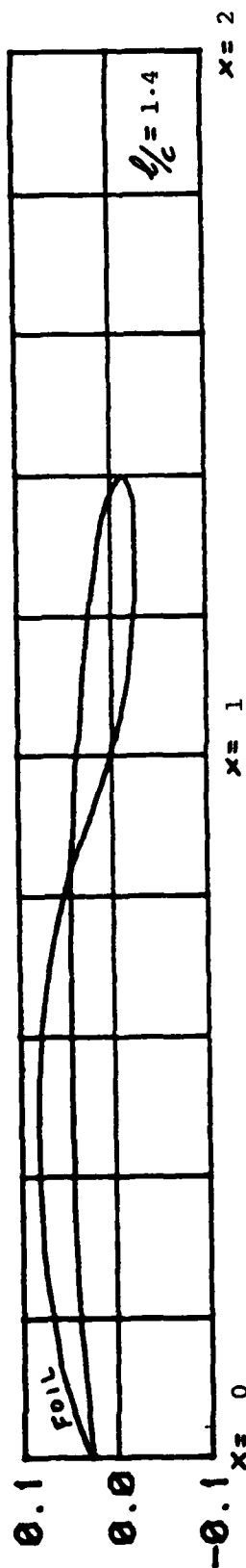
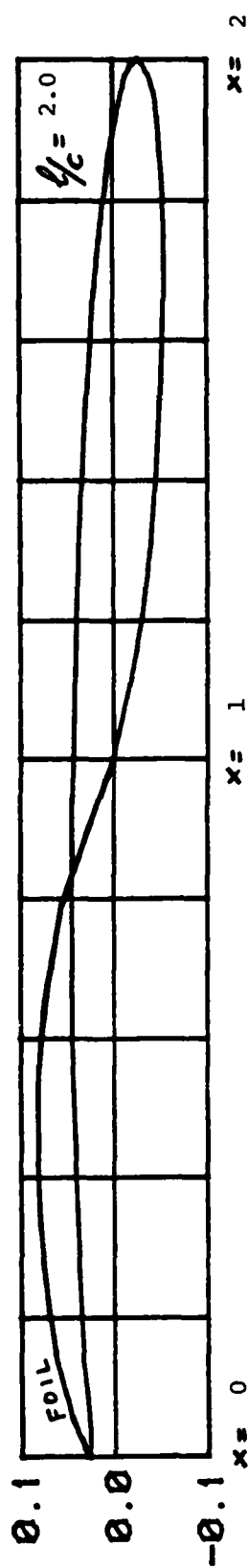
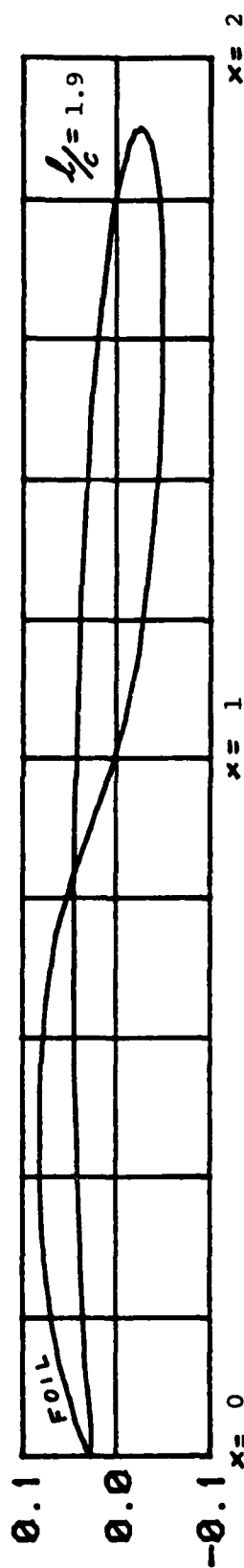
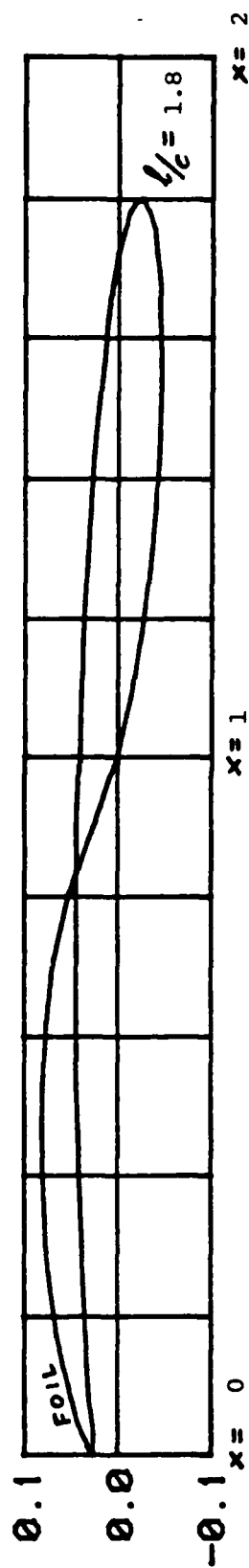
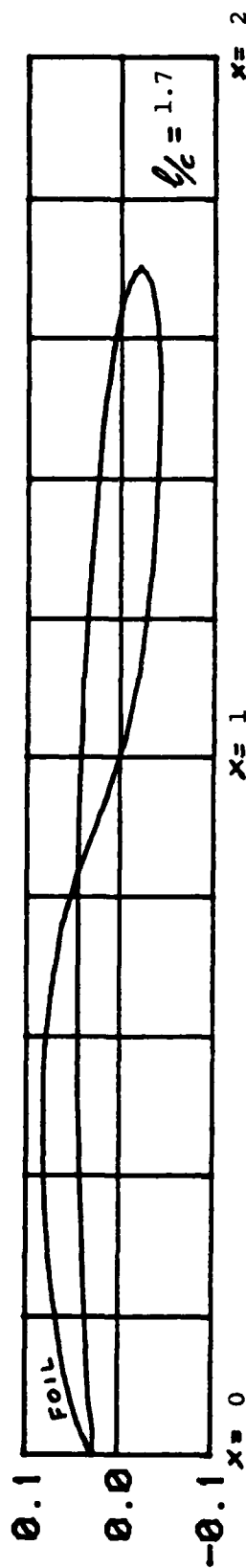


FIGURE 7b

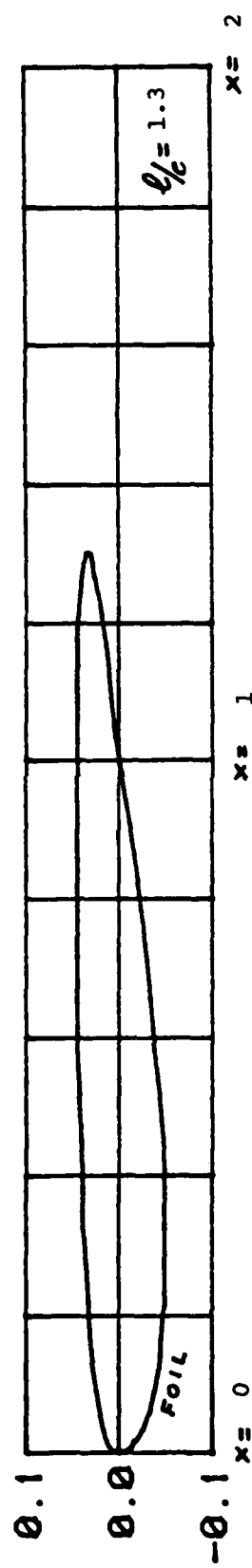
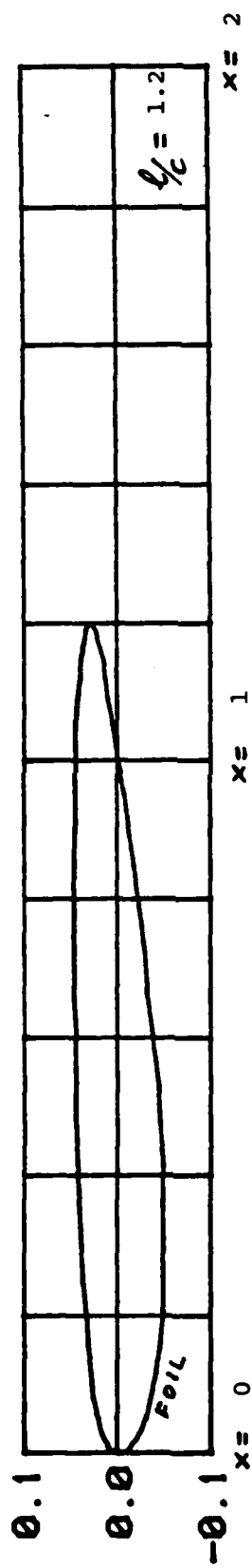
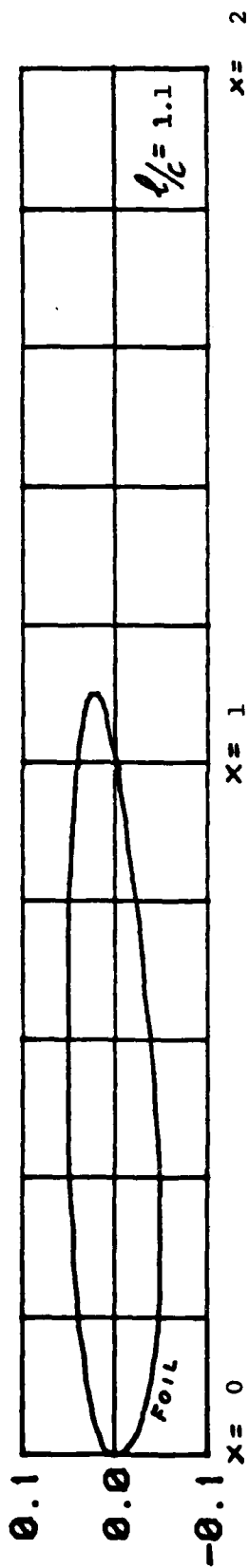
NACA $a = 0.8$ ($h_{max}/c = 0.0679$) at $\alpha = \alpha_i$



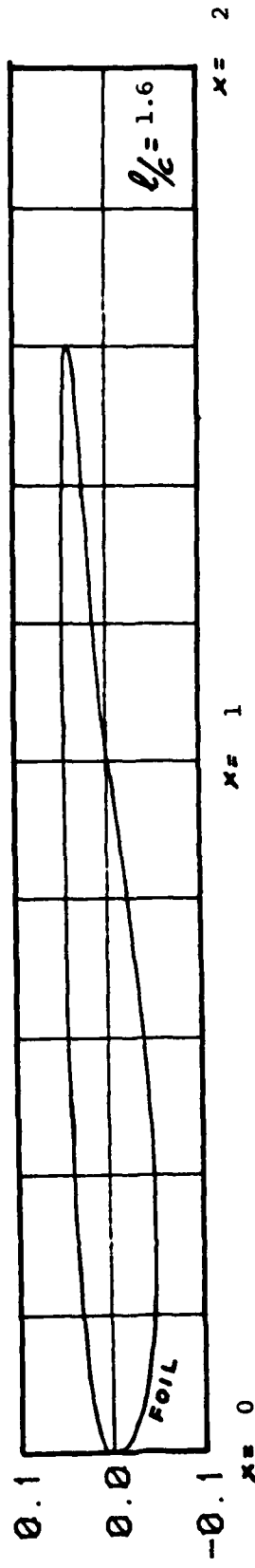
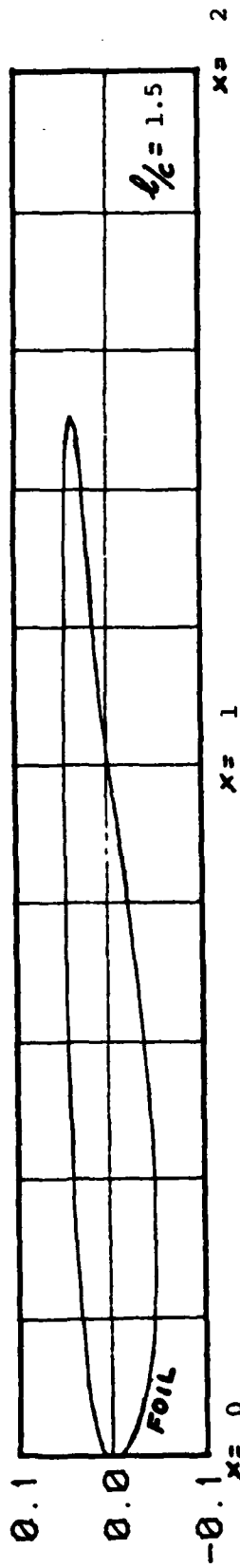
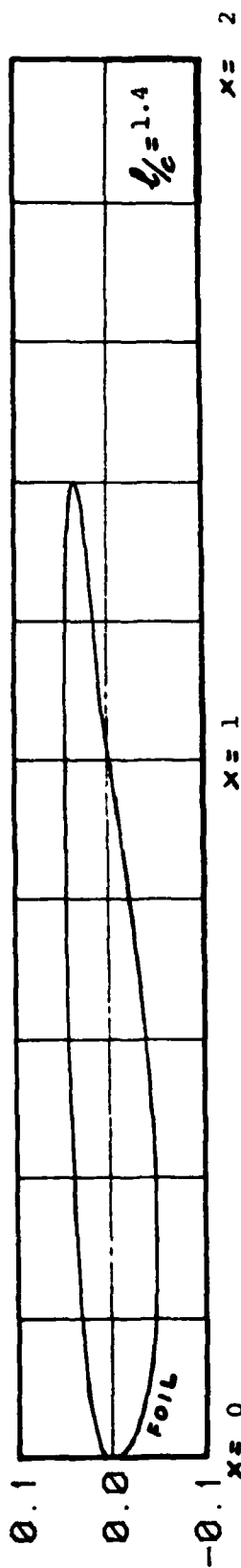
NACA $a = 0.8$ ($f_{max}/c = 0.0679$) at $\alpha = \alpha_i$



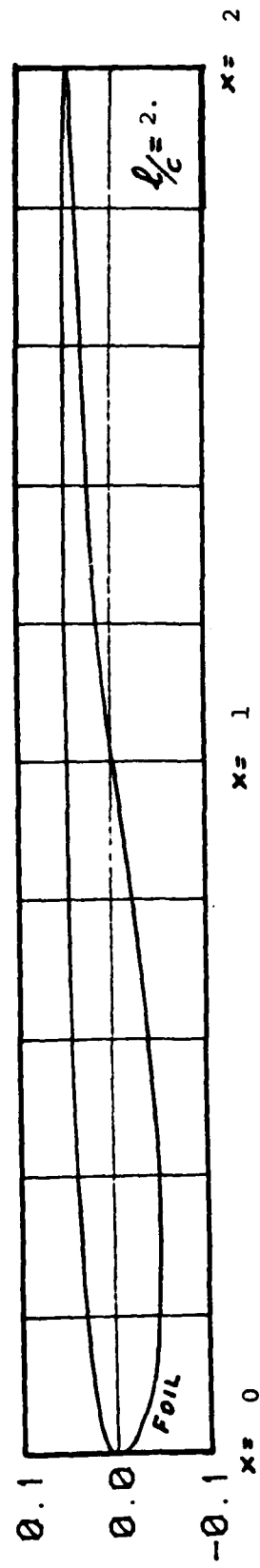
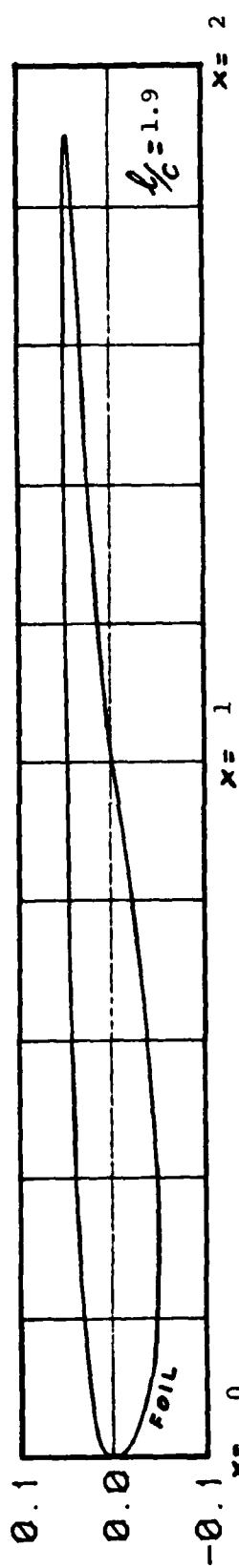
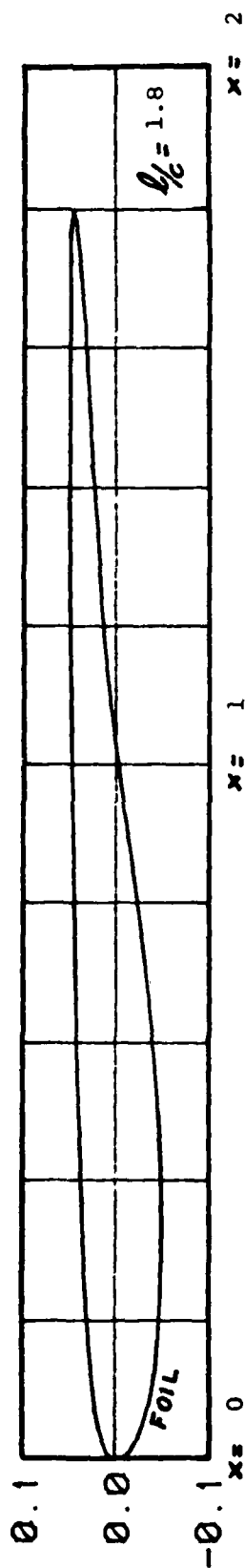
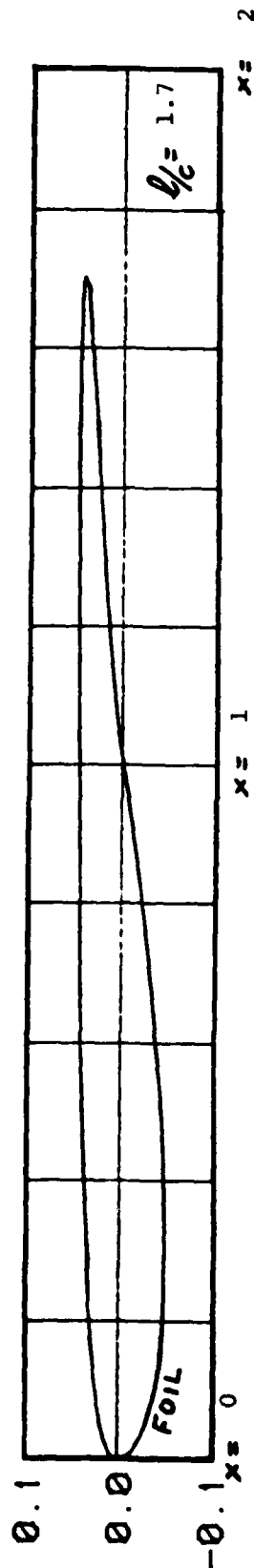
NACA 0010 THICKNESS FORM AT $\alpha = 0^\circ$



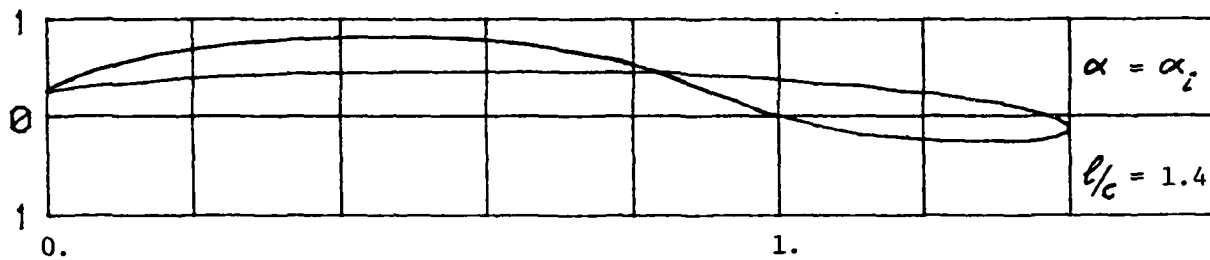
NACA 0010 THICKNESS FORM AT $\alpha = 0^\circ$



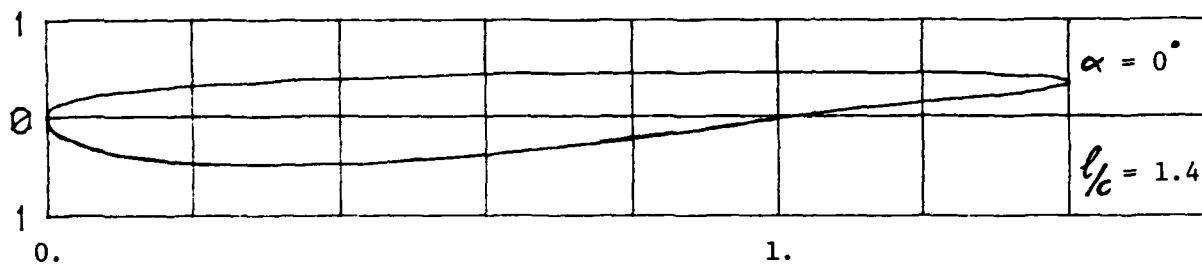
NACA 0010 THICKNESS FORM AT $\alpha = 0^\circ$



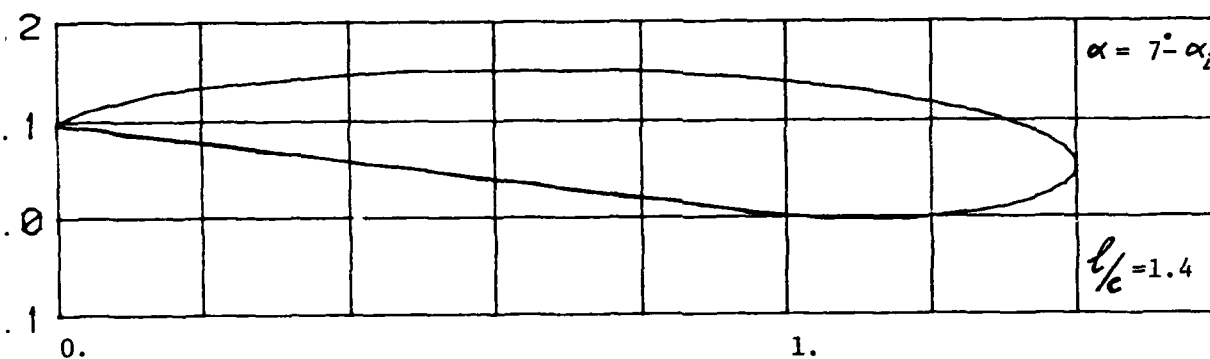
NACA $a = 0.8$ ($f_{max}/c = 0.0679$)



NACA 0010



FLAT PLATE



NACA $a = 0.8$ and NACA 0010

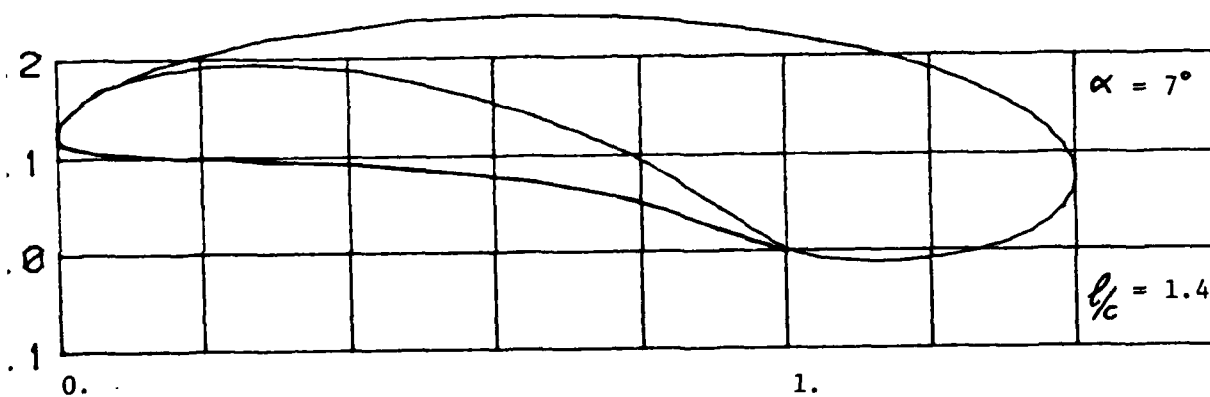


Figure 9

THE THREE ELEMENTARY PROBLEMS

FOR NACA $a = 0.8$ COMBINED WITH NACA 0010 AT $\alpha = 7^\circ$

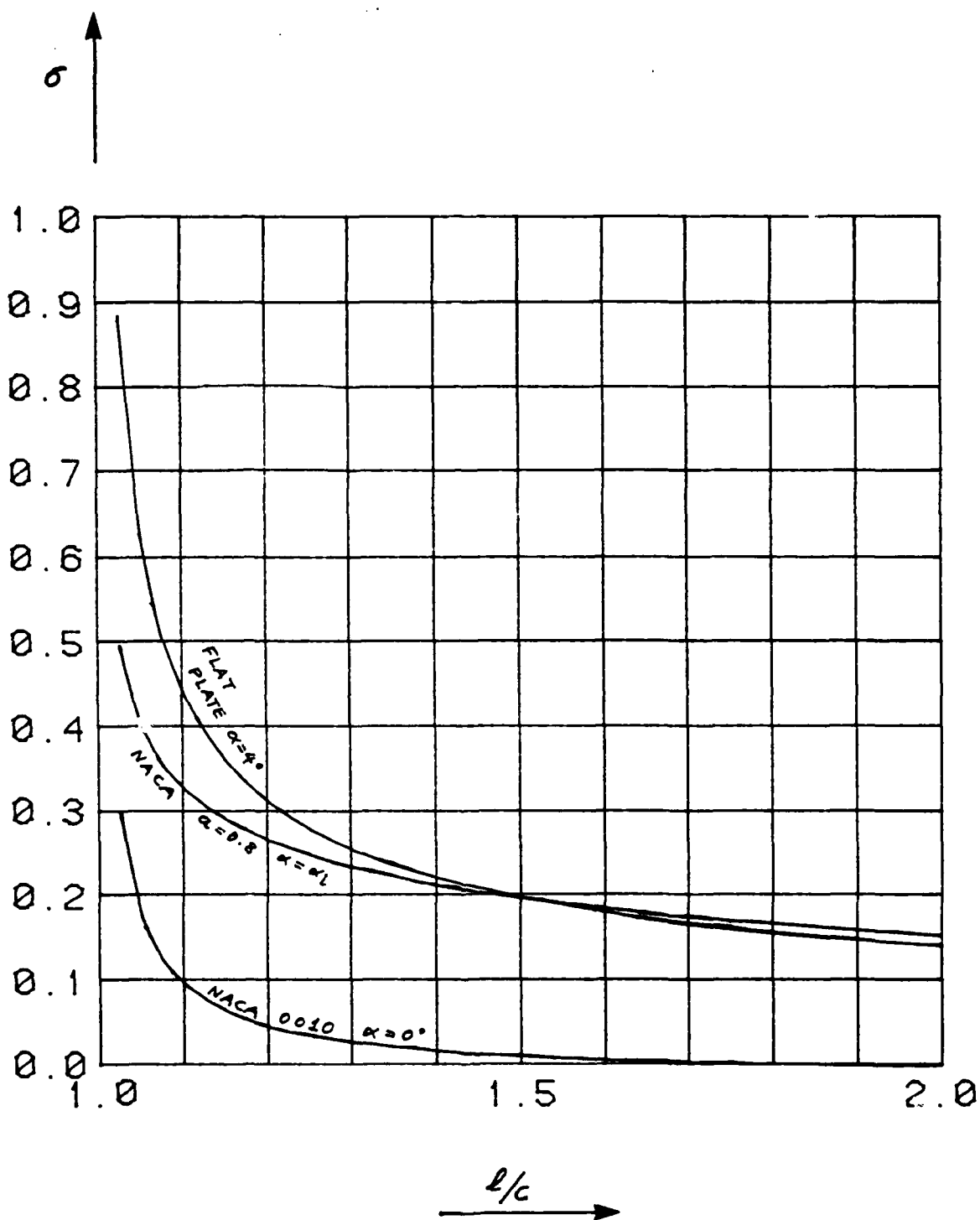


Figure 10

CURVES OF σ VERSUS l/c FOR SOME HYDROFOILS

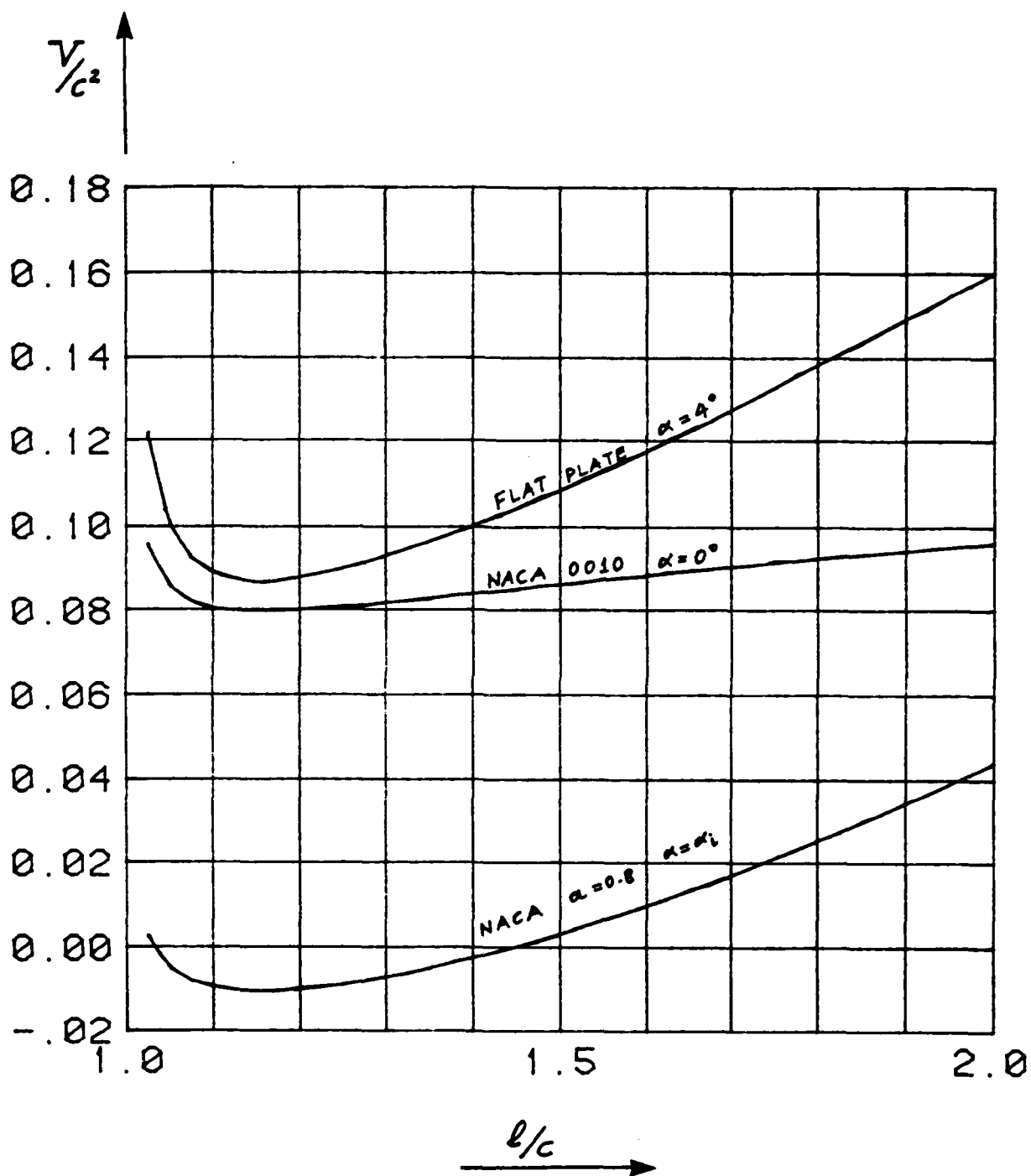


Figure 11

CURVES OF V/c^2 VERSUS l/c FOR SOME HYDROFOILS

END

FILMED

9-85

DTIC